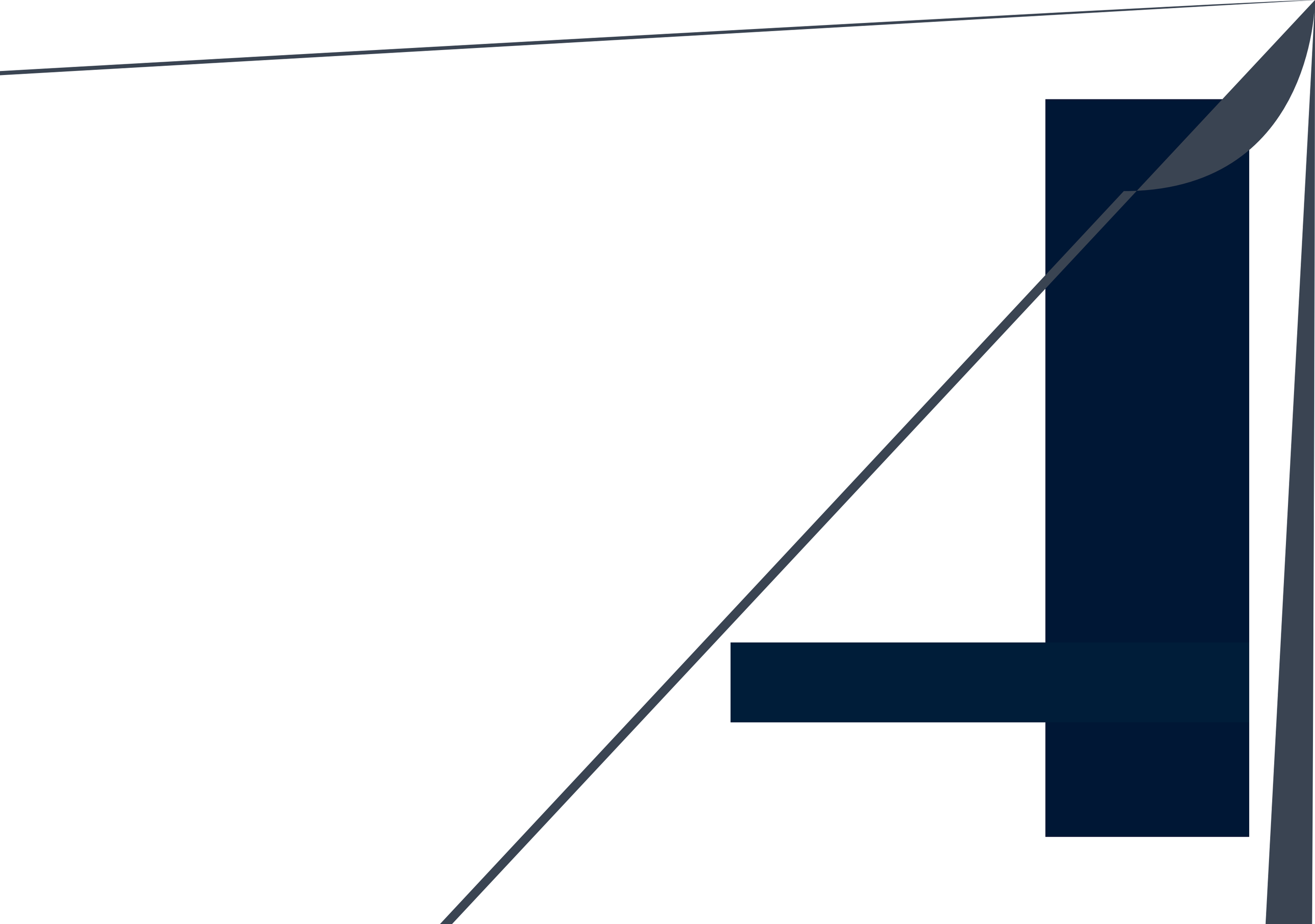

18650

611731

18650 :

B D A B C

0 0 1C/3C A B D 1 000

( ) A2
NMP (Celgard2300) PVDF(HSV900)
CMC SBR 10 μm
16 μm

1.2

1

		%		(g/1540.25mm^2)		%	(g/1540.25mm^2)	(μm)	(μm)
A		94.00	Super-P	0.325	A2	97.50	0.136/0.145	A1	15	16
B	:=9:1	94.00	Super-P	0.33	A2	97.50	0.136/0.145	A1	15	16
C	:=9:1	94.00	Super-P	0.33	A2	97.50	0.136/0.145	A1	15	16
D	:=9:1	94.00	Super-P	0.33	A2	97.50	0.136/0.145	A1	15	16

1.3

1 A
PVDF 95% 2% 3%
16 m

2 B
+ 9 1 PVDF 95% 2% 3%
16 m

3 C
+ 9 1 PVDF 95% 2% 3%
16 m

4 D
+ 9 1 PVDF 95% 2% 3%
16 m

5 A2 CMC SBR
94.5% 1.5% 2.5%
10 m

18650
18650

2

2.1

2

	%			
	A	B	C	D
2A	100.00	100.00	100.00	100.00
6A	99.40	100.10	98.80	99.30
8A	99.10	100.60	97.50	100.00
10A	98.40	100.80	92.60	100.60
15A	89.50	100.10	57.90	100.10
20A	59.60	100.10	31.10	99.20

2 B D
20A
100% A
20A
60% C 20A
30%

B C

5%

D

A

2.3

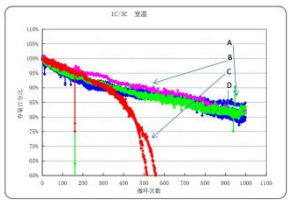

(a) 1C/3C

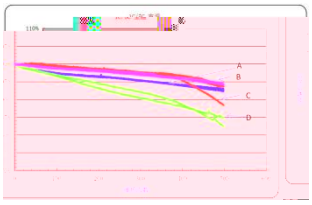

(b) 1C/5C

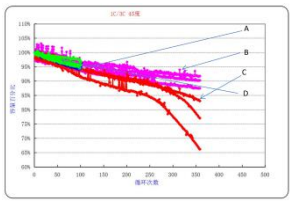

(c) 45 1C/3C

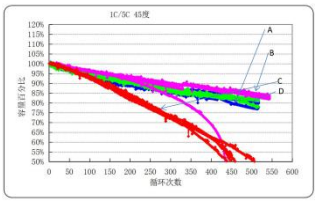

(d) 45 1C/5C

1

45

1C 3C 5C

1 1C/3C A

B D

1 000 C 300

45 1C/3C

45 1C/5C

C

3

55

3.1

4

(g)

(V) (C) (V) (V) (min)

A	10	0.7	9.998	3.403	240.000	No	46.290	46.288	No	No	Pass
B	10	0.7	9.999	3.442	240.000	No	46.269	46.268	No	No	Pass
C	10	0.7	10.018	3.417	240.000	No	46.494	46.492	No	No	Pass
D	10	0.7	10.024	3.445	240.000	No	46.065	46.062	No	No	Pass

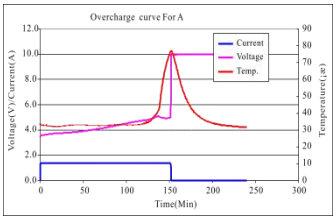

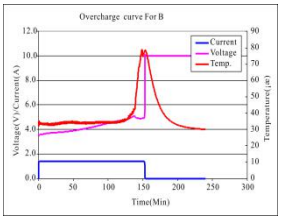

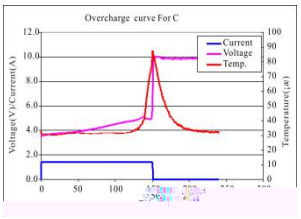

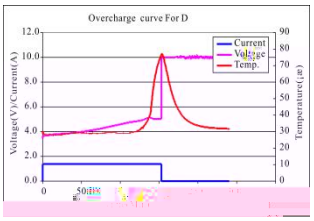

2

120 SEI

200

4 2

70~80

4

3.2

5

S/N	(C)	(V)	(V)	(A)	(min)	(Ah)				
A	1	4.202	-1.315	-2.000	150.000	1.071	No	No	No	pass
B	1	4.204	-1.331	-1.999	150.000	1.072	No	No	No	pass
C	1	4.202	-1.388	-2.000	150.000	1.062	No	No	No	pass
D	1	4.202	-1.320	-2.001	150.000	1.070	No	No	No	pass

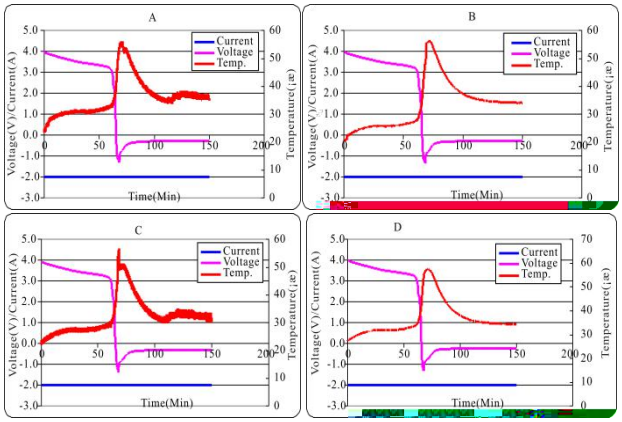

3

5 3

60

50

55

5

3.3 55

6

	(V)	(mΩ)		(g)						Result
A	4.171	0.220	20.90		51.240	49.051	115.8	Yes	No	No	Pass
B	4.169	0.218	20.60	≥	51.124	48.979	108.1	Yes	No	No	Pass
C	4.167	0.011	21.40	250Ω	50.795	50.794	113.4	Yes	No	No	Pass
D	4.168	0.005	20.70		51.734	50.024	108.3	Yes	No	No	Pass

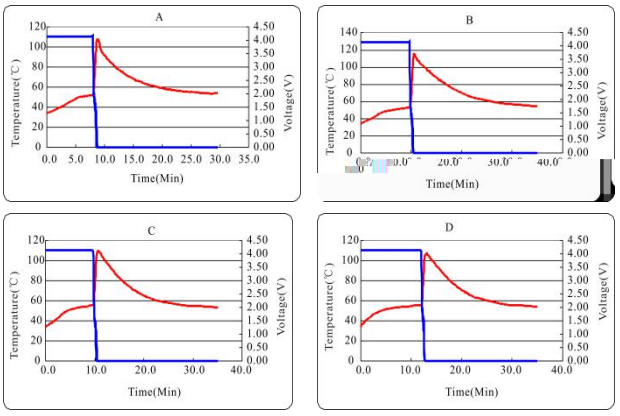

4

6 4

120

4

18650

1 B D

C

2 A B C

D

3 1C/3C A B D

1 000 C

下 8

SHEPWM

MATLAB

:

TM 46 A 1001-9006 2022 02-0005-04

Research on Optimizing Selective Harmonic Elimination Pulse Width Modulation for Three-level Inverter

WANG Zhengjie, CUI Yu, ZHANG Xiao

(DEC Academy of Science and Technology Co., Ltd., 611731, Chengdu, China)

Abstract: This paper does research on the three-level selective harmonic elimination pulse width modulation strategy, and deeply analyzes the key technologies such as the principle of waveform synthesis, the method to obtain the initial value, the iterative steps of switching angle trajectory, and so on. Furthermore, an optimization method and corresponding algorithm are proposed to improve the harmonic performance of inverter's output voltage. Finally, this paper verifies the effectiveness and practicality of the proposed strategy through MATLAB numerical simulation.

Key words: selective harmonic eliminated pulse width modulation (SHEPWM); three-level inverter; harmonic performance

ضي W ⁚⁚ à ا à ´ ˆ ˇ ˙P ﻫ № ч ˇ

Z ĭ ì Ţ ˇ ì Z ⌠ ₩ ˇ U ˇ

ск Ð Y ĭ °° └ ˇ ˜ ⌠ п ˜ ↓ ˇ ₹ ا

ч └ ì W ٦ غ [1-2] Âч ২ ٧ └ Â G SHEPWM ˆ └ W ск Ð

˜ ˇ ₩ ˆ Y ˜ ˇ ٧ W ск ضي ا ق ˜ ṗ ¯ ƀ ⊥ ˇ غ ˆ Y ضي □

Ð Ţ [3-4] ɜ ₩ ˇ ˆ Y ɲ PWM ˜ Й ˇ ì ɾ └ ٧ ˇ

└ ˇ ضي □ └ ╠ Й ˇ ٧ ا ق ск ɾ ₹ ا ˇ ٧ ´ ʊ ск

Ð ˜ ˇ ɾ ٧ ˜ ė °° Â

Â ɣ ĭ ск ч ɒ ˇ SHEPMW

˘ (Selective Harmonic Ţ ĭ ا à Δ ˜ ŭ à

Elimination PWM, SHEPWM) ₩ ĭ ск ٦ ˜ ƀ Â ₹ ₩

PWM ɲ [5-7] ì h ا ĭ ск Y ĭ (Total Harmonic Distortion, THD)

₹ ا ị ˆ ĭ ˇ ⌠ ˜ G ˜ ị ٧ ч Ð ɲ ˘ ˇ

' 2022-03-16

' ^ 1991 ˜ ˇ ˇ 2016 ʒ G ´ ĭ ɲ ск F ʒ ˇ ˇ Â ضي ĸ غ

Ė ˜ z h ɾ Hu ĭ ск o ь └ à ɒ ŭ ƀ Â

ㄱ Δm ĺ. ν ˘ ˆ γ ض ѽ ㄱ
Â
ŭ N = 7˜ Δα = 3° Ė ˆ 5˜
⌈ m = 0 ㄱ Δ ν α⁰ = [42°, 48°, 57°, 63°, 72°, 78°, 87°⌋ U ŭ Δm = 0.005 ㅑ № ˘ m ㄷ 0 h 1.15 ˘ ≠ Matlab Ţ fsolve ₱
˘ ⌈ m ŗ [0, 1.15] ㅎ ṗ
˝ L ĺ. ㅈ 3 Â

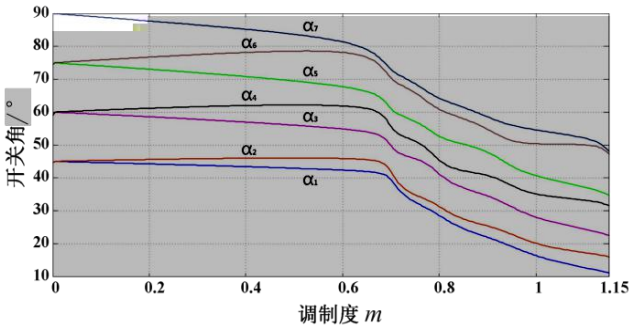

3 PWM

ㅑ ↻ Ḡ ⌈ ˝ ضي ⁘
˘ Ð' α1<α2<…<αN Â ⁘ ㅈ˜
˘ ⁘ Ð m ν ضي 1.15 ˚ Â
ㅅ L M = UL-L / Vdc = m ¦ 1.732/2 ≈ 1˜
ㅊ SHEPWM L˜ γ Ь D SVPWM
L ₩ ㅅ ≠ Â

3

D SHEPWM Ţ
Ð ᵩ ν ㅑ 0˜
№ ŋ ˘ ₩
˜ ˇ ˘ Ƈ Ḃ Ψ
ᵠ˘ . Ь ≠ G´ ᵾ ᄀ Â
ㅑ ˘ ∓ ↻ ₩ ŋ ˇ ˘
Ð˘ ㅅ ˇ ╠ N-1
˘ ㅑ ضي ㅎ ṗ ∓ ㅅ
ĺ (Total Harmonic Distortion, THD) ㅛ Â ˘
˘ ⌈ Ѝ ↓ Ė '

$$\begin{cases} \min\limits_{\alpha} \sqrt{\sum\limits_{k}\left(\dfrac{f_k(\vec{\alpha})}{f_1(\vec{\alpha})}\right)^2} \\ f_1(\vec{\alpha}) = m \cdot \dfrac{V_{dc}}{} \end{cases} \quad (6)$$

Ţ' 0<α1<α2<…<αN<π/2˜ 5<k<N2 ғ k Ь ㅑ 3
Ò ˘ N2 ㅑ (N2>3N-2) Â
Ꮆ Ð ν
˘ ㅐ ╠ ∓ ˝ Δ ν Ь Ṕ ˘
ㅊ ∓ ₩ ㄱ ˘ Ĭ r
Ѝ'
(1) ㄱ Δ ν ㅑ D SHEPWM Ţ
L m Ѝ ˝ Â
(2) ѽ N2 ㅑ 3N˜ ⁘ Â
(3) Ṕ Ɒ N2 = N2 + 2˜ ⁘ ⌈ ˝
ƀ ㅑ ㄱ Δ ν˘ Ṕ ⁘ Â
(4) (3) ⌈ N2 = N2*(ν) Â
ĭ Ţ ν ˘ n-1 ƀ ㅑ n
ㄱ Δ ν ˆ ∓ Ь ' ˘
ˆ γ n-2 n-3 ƀ ㅑ Δ ν
Â
Ş ↑ Matlab ĺ ⁘
˘ ⌈ ↻ m=1.0˜ N=7˜ N2=33
˘ ŋ ╠ ɕ ŋ U ˝ ˘ 1 Â
1 m=1.0

ˆ	1	2	3	4	5	6	7
ŋ ╠	16.3	20.1	28.1	35.1	40.7	50.4	54.6
ŋ U	24.6	27.1	32.7	36.8	40.9	46.6	49.0

ㅈ 4 ɕ ㅈ 5 №≠ ∓ ↻ ŋ ╠ U ㅅ
PWM № ㅈ Â ˆ γ ∓˘ ضي D
SHEPWM Ţ˘ ˆ ˘ ㅑ 3 ¦ 7
2=19 ˘ G 19 3 Ò № خش
ض ˘ ₩ 19 Ƈ Ḃ
ᵠ˘ h Ţ ضي 25 ˚ Â ضي ŋ U
SHWPWM Ţ˘ ㅛ № ᵠ˘ ᵖ h
№ Ţ ضي G 35 ˘ W ض
↻“ ” Â
U ⌈˘ ╠ 35 THD˜ Ь´ Ƈ 3
Ò ˜ ㄷ ㅅ 39.5% Ѝ 15.03%˜ ŋ
Â ˘ ضي □ ˝ Ѝ˘
ˆ ض ، ∓ ㅅ ˘ ㅛ
ᄀ ɕ Â

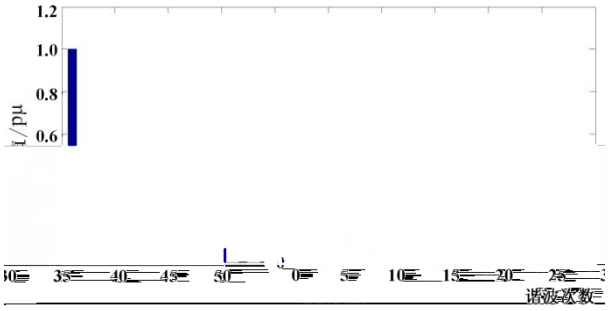

4 SHEPWM FFT (m=1.0)

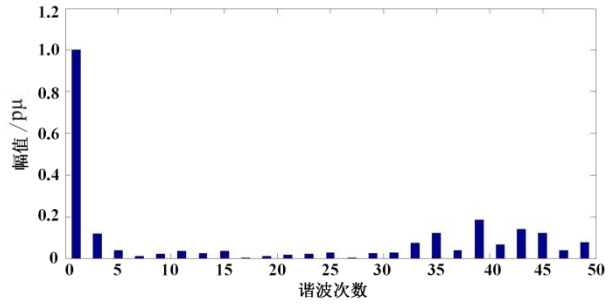

5 SHEPWM FFT (m=1.0)

4

№ SHEPWM L ~ Ţ Δ ů à ţ

THD MATLAB SHEPWM

[1] , . [J]. , 2011, 26(1):92-99

[2] Blaabjerg F, Chen Z. Power Electronics for Modern Wind Turbines[J]. Synthesis Lectures on Power Electronics, 2006, 1(1):1-68

[3] . ~ [J]. , 2011, 26(9):167-174+189

[4] , , . β [J]. Ţ , 2011, 31(30):30-38

[5] , . SHEPWM № [J]. , 2011, 26(9):183-189

[6] , , SHEPWM [J]. , 2004, 19(1):16-20+54

[7] , , SVPWM SHEPWM L [J]. Ţ , 2007(16):72-77

[8] . SHEPWM [D]. , 2012

上 4

300 № Â 45Ņ 1C/3C 45Ņ 1C/5C Ä

Ţ à à à

[1] ↔ . Ь [J]. , 2011, 35(1): 12-14

[2] . № [J]. ş , 2019 (8):39-41

[3] , , . Ь [J]. , 2020, 44(9):1383-1386

[4] , , . Ħ № [J]. , 2017, 47(6):347-350

[5] , , . Ħ Ь [J]. ş , 2021, 25(3):136-142

[6] , , . Ħ [J]. , 2018, 42(3):343-346

[7] , , . Ħ [J]. , 2019, 43(7):1223-1225+1229

[8] , , . NCM Ħ № [J]. ~ 2020, 41(6):881-887

[9] , , . 18650 [J]. Ţ ~ 2017, 27(7):1602-1607

[10] Ħ , ↔ , . Ь β 18650 [J]. , 2021, 21(1):124-132

[11] , , . 18650 [J]. , 2019, 43(1):67-70

[12] . 18650 Ħ L [J]. 2020 (12):17-18

[13] , , . NCR18650A Ħ Ь [J]. , 2020, 8(6):455-461

1,2 1,2 1,2 3

/, ǍȻ 4//51/ 0, E ę Å˝ 4//51/

1, 4//51.

“ ”

TP274 A 1001-9006ˆ 2022˜ 02-0009-07

The Overview of Information Security, Network Security and Cyberspace Security

ZHANG Yufei [1,2], *CHEN Hong* [1,2], *ZHAO Chenyu*[1,2], *CHEN Ting* [3]

(1. Energy equipment Cyber security Key Laboratory of Sichuan Province, 611731, Chengdu, China;

2. DEC Academy of Science and Technology Co.,Ltd., 611731, Chengdu, China;

3. University of Electronic Science and Technology of China, 611730, Chengdu, China)

Abstract: The development of information technology is accompanied by a steady stream of security problems. At different stages, the concepts "information security, network security and cyberspace security" were proposed to describe these problems. These three concepts intersect in various materials, and their specific connotations and logical relationships are not clear. In order to clarify the relationship between the three concepts, this paper elaborates on their origins, definitions, and research objectives, explores the main differences in the security problems faced by different periods, and introduces the corresponding key technologies.

Key words: information security; network security; cyberspace security

ɾ Ḥ ʁ ˘ ɳ Ḃ ʁ ₹ ˘

' 2022-04-21

' ضه ሳ ŭ ' ɳ ŵ ɾ. Ḡ ˀ Ь ŭ’ ˆ ' 2019YFG0534 Â

' (1994ˊ ǰ ˘ 2020 ʒ ɢ Ғ ʒ˘ Â ض ɣ فج ˋĒ̃ h ɾ Hʊ ɳ ƀ Â

[1]

1.1

Caesar

16

19

1949

1985 12

TCSEC

1999 12 ISO

2005 ISO 27000

1999 9

GB 17589-1999

2001 ISO/IEC 15408

GB/T 18336-2001[3]

2002-2006

GB/T 18238 GB/T 15843

1.2

ISO 27001:2005

[4]

[5]

[6]

1.3

1

ŋ ɇ ⅵ
˘ № h ɣ ŭ Ḥ
Â ь № ε ˘ ǐ ε ɯ
˘ ˜ □ ˫ ŭ Â ᴰ ь
˜ №ч ң ˈ ɢ ɇ
Â´ № à O à ɢ
≠ ь [7]Â
ˆ 2˜ L ˈ L
˫ ˘ aˌ.. ضˌ..
Ḡ Ḥ ь
ą ɇ Â ŋ №ч h L
ˆ Discretionary Access Control, DAC˜ ɇ L
L˘ Mandatory Access Control, MAC˜ ң [8]Â
ɢ DAC ʏ ɇ MAC ь Ḡ
˘ ∓ ↄ ɢ L ﷺ Role-Based
Accesss Control, RBAC˜ [9]ʏ ɣ ь □ à
˜ ɇ ʅ ң ǐ L˘ ˫
ض ч Â
ˆ 3˜ Ḥ ˈ Ḥ ˝Ḥ ɣ ⅵ
ŋ ᴰ Ḥ Ḥ Ḥ [10]Â
Ḥ № h ˜ ǐ à ≠ à ɇ
[11]ʏ Ḥ ˜ Ḥ ⁰⁰ ⅈ ﷺ ɇ Ḥ
ﷺ ˘ h ´ Ḥ ﷺ ɇ ﷺ ’ Ḥ
≠ ɇ ɳ № ˘ ˆ
Ḥ ˝˫ à ⅈ ˘ ǐ ᵣ ≠
№ à Ḥ № à ˝˫
à à ɳ № ’ Ḥ
ą Ḥ ƀ ч Ḥ ɛ ˘ Ḥ
№ч . ɇ . ң Â Ḥ
´ à Ḥ ﷺ à
’ Ḥ ´ Ḥ à L à
ɇ ˘ ɢ Ḥ ɣ ˘ ₩ L Ḥ
ʐ ﷺ Ḥ ᴰ ʐ˘ ´
ɐ à [12-13]Â
ˆ 4˜ ˆ Ḥ ˈ ˆ Ḥ ɾ à
ɒ ɇ ƀ ˌ.. ŭ Ḡ
Ḥ ŋ Â ISO/IEC 15408 ‰ ɣ˜ Ḥ
ч' ă ь ɒ à ƀ ضˌ к ɒ Й
˜ ˘ ɇ [14]Â˜ Ḥ
˜ ѽ ₩ ɷ Ḥ к ˘ Ꝑ
₩ Ḥ к ˘ ɾ Ḥ к ⌠ ɒ ˜ à ƀ
à Ꝑ ⌠ ˘ ₩ ₩ ˘ ₩ Ḥ к ₩ ˘ ɾ
Ḥ к ⌠ ɷ [15]Â˜ Ḥ ˜
h ´ ˜ Ḥ ɒ ˜ à˜ Ḥ ˜ ﷺ à
ɒ à Ḥ к ɇ Â ɯ ˜ Ḥ
˜ ɣ ʮ ŋ ˜ ˘ З˜ ɢ
Ḥ к ɾ ˜ ᵈ ˜ Ḥ Â
20 ь 70 ɳ U˘ ŭ ą
ض Ꞇ˘ ǐ ⌠ ↄ ŋ ˘ Ḥ
ŋ ɾ Ḥ h ь Ꞇ Â

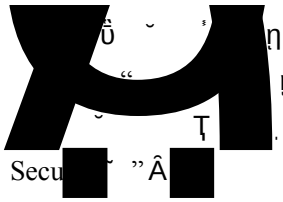

“ ” Cyberspace Security “ ” Network Secu ”

2.2

Network security

ISO/IEC 27033-1:2015

/ VPN [22]

1

[18]

“ ” “ ”

[19]

[20]

[21]

2.3

№

12

1

3.1

21

2003

2011

2012

2016 11

Cybersecurity Law of the People's Republic of China

2012

ISO

2012

ISO/IEC 27032:2012

[24]

2020

ISO/IEC TS 27100:2020

[25]

3.2

ISO/IEC 27032 2012

ISO/IEC 27000:2009

information security

"in the Cyberspace"

"Cybersafety"

Cyberspace Security

Cybersecurity

Cyberspace Security

Network Security

1948

(cybernetics)

Kubernetes

(rudder steersman)

cyber

[26]

ISO

cyberspace

[25]

[23]

ˆ 3˜ ŋ ˜ h ´ Ơ Й ˈ
ŵ № Ч Ь ŋ ´ ˘ Ḡ
Л ↕ ˘ № Ч ė № Ч ˘ № Ч
ң ╠ ė D ’ Ŷ Ң
ė ч ŋ № ˘ ´ ŵ ė
ŋ à ч ҕ № ǐ̋
’ ŷ ˘ ´ Ơ
à à U ’ Ÿ
Ь ’ Ź Â
ˆ 4˜ ŋ ǐ̋ ˜ ė ˜
Ḡ Â ╠ Ḡ ˆ №
ч ң ҩ h' ɢ ǔ̈ Ḡ ė
Ḡ Â ˘ Ь ŵ
ė ث ш Ӟ ȝ h Â
ˆ 5˜ Ḡ ŋ
Â à Ɛ à ė
ǔ̈ ˘ Ь ˘ à
h Ɛ ŋ ▯ ѵ à˜

1, 2 1, 2 1, 2

1. 611731 2. 611731

MATLAB/Simulink

MATLAB/Simulink

TP274 A 1001-9006 2022 02-0016-05

Design of Active Disturbance Rejection Controller for Turbo-generator

ZHOU Yunhong[1,2], *SANG Zi*[1,2], *LIU Sisi*[1,2]

(1. Energy equipment Cyber security Key Laboratory of Sichuan Province, 611731, Chengdu, China;

2. DEC Academy of Science and Technology Co.,Ltd., 611731, Chengdu, China)

Abstract: In order to solve the problem that the slow response of the traditional speed control adopt on turbo-generator which cannot effectively suppress the emergency response caused by the load change on the grid side, a speed controller based on active disturbance rejection control is proposed. First, in order to evaluate the operating conditions of the turbo-generator in various environments accurately and quickly, a simulation model of the turbo-generator is built in the MATLAB/Simulink simulation environment. Secondly, the speed control logic is optimized by the control method based on the active disturbance rejection control to reduce unnecessary emergency control actions, which improves the operation efficiency. Finally, the transient-steady state of the turbo-generator is simulated and analyzed. The simulation results show that the turbo-generator adopt the active disturbance rejection control can quickly recover stabilize while the grid side load changes, which means the speed can be quickly stabilized after fluctuating within a very small range, reducing the probability of triggering emergency control, and effectively improving the operating efficiency of the turbo-generator.

Key words: turbo-generator; active disturbance rejection control; emergency control;MATLAB/Simulink

[2]

[1]

DEH

Automatic Generation Control AGC

Coordinated Control System CCS

2022-04-21

2019YFG0534

(1994) 2021

[3]

[4]

[5]

Generalized Dynamic Fuzzy Neural Network

GD-FNN

[6]

[2]

[7]

¾ ثم ض

ή

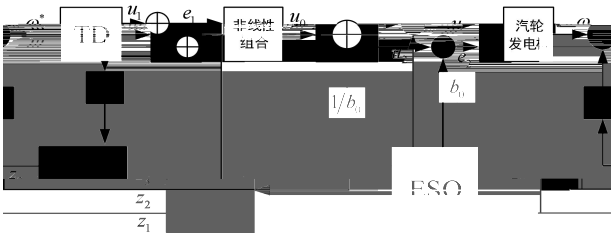

2

3.1

M_{st} M_{em} M_f

PID

:

$$J\frac{d\omega}{dt}=M_{st}-M_{em}-M_f \quad (4)$$

J

e u_0
fh $fhan\ e,v_2,r_0,h$
u_1 u_1 $h\bullet v_2$ (6)
u_2 u_2 $h\bullet fh$

2.5

u_1 u_2

r

h $fhan\ x_1,x_2,r,h$

$$\frac{V_{fd}}{e_f}=\frac{1}{K_e+sT_e} \quad (5)$$

V_{fd} e_f K_e

T_e

d rh^2
a_0 hx_2
y x_1 a_0
a_1 $\sqrt{d\ d\ 8|y|}$ (7)
a_2 a_0 $sign\ y$ a_1 d /2
a a_0 y $fsy\ y,d$ a_2 1 $fsg\ y,d$
$fhan$ $r\ a/d$ $fsg\ y,d$ $rsign\ a$ 1 $fsg\ a,d$
$fsg\ x,d$
$fsg\ x,d$ $sign\ x$ d $sign\ x$ d /2 (8)

3

[9]

3.2

“ ”

[10]

,

b_0, 1, 2, 3

ADRC 2

$$e \quad z_1 \quad y$$

$$fe \quad fal\ e,\frac{1}{2},d$$

$$fe_1 \quad fal\ e,\frac{1}{4},d \tag{9}$$

$$\begin{aligned} z_1 &\quad z_1 \quad h\ z_2 \quad {}_1 e \\ z_2 &\quad z_2 \quad h\ z_3 \quad {}_2 \bullet fe \quad b \bullet u \\ z_3 &\quad z_3 \quad h \quad {}_3 \bullet fe_1 \end{aligned}$$

$$fal(e,a,d)=\begin{cases} \dfrac{e}{\delta^{a-1}}, |e|\le d \\ |e|^{b}\ sign(e), |e|>d \end{cases} \tag{10}$$

y

z_1 z_2 z_3

u ADRC

b_0, $_1$, $_2$, $_3$

3.3

TD ESO

$$\begin{cases} u_0 = k_p\, fal(e_1,\alpha_1,d)+k_d\, fal(e_2,\alpha_2,d) \\ e_1 = u_1 - z_1 \\ e_2 = u_2 - z_2 \end{cases} \tag{11}$$

ESO

3

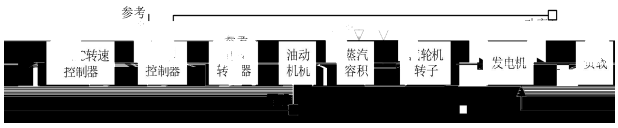

3 ADRC

4

ADRC

Matlab/Simulink

4

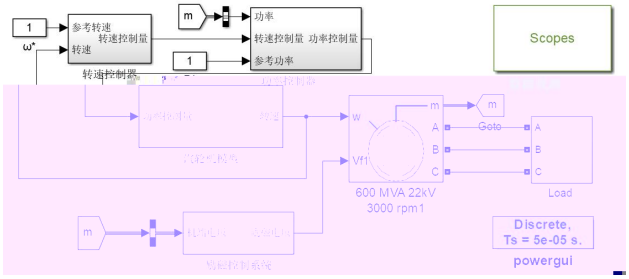

4

1

/W	600E6
/V	22E3
/Hz	50
/V	0

ADRC

PI

4.1

5 6 ADRC

PI

3 000 r/min ADRC

PI

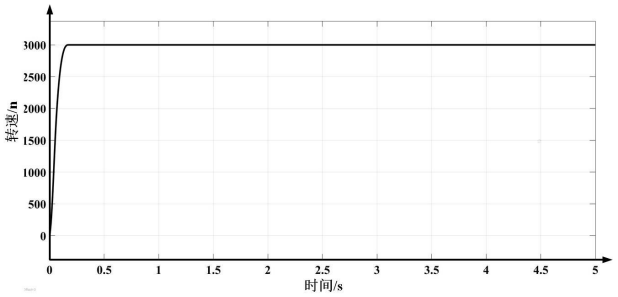

5 ADRC

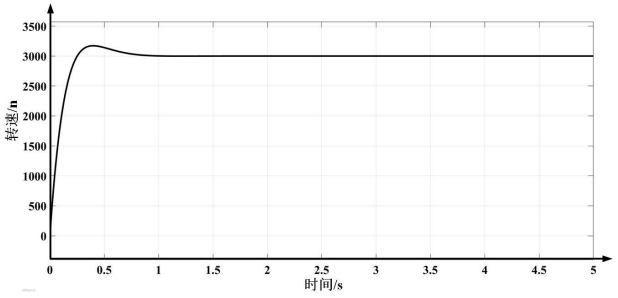

6 PI

4.2

7 8

ADRC

PID

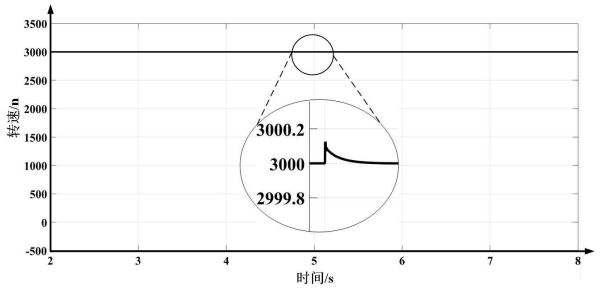

7 ADRC

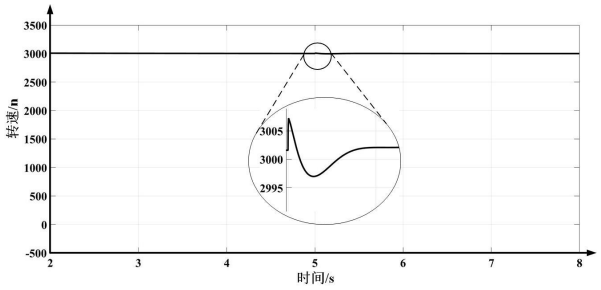

8 PI

5

[1] , , .
[J]. , 2021(6):5-8

[2] , , .
[J]. , 2020, 41(9):1312-1319

[3] , , . [J]. , 2021, 35(4):6-11

[4] , , . PID [J]. , 2020, 15(S1): 149-156

[5] . [D]. ( ), 2007

[6] . [J]. 2008, 30(11):86-89

[7] , , .
[J]. , 2020(10): 219-222

[8] .
[J]. , 2018, 32(2):15-20+28

[9] Han J Q.From PID to active disturbance rejection control[J]. IEEE Transactions on Industrial Electronics, 2009, 56(3): 900-906

[10] . —
[M] : , 2008:255-261

上 15

[22] , , . [J]. , 2012, 35(4):109-112+116

[23] . [J]. , 2018(9):54-57

[24] ISO/IEC 27032:2012, Information technology — Security techniques — Guidelines for cybersecurity[S]

[25] ISO/IEC TS 27100:2020, Information technology — Cybersecurity — Overview and concepts [S]

[26] . (cyberspace) [EB/OL]. https://xueshu.blogchina.com/606177333.html

[27] , . [J]. , 2019, 5(3):4-18

[28] , , . [J]. : , 2016, 46(2):125-164

[29] , , .
[J]. , 2019, 43(4):495-504

[30] , , . [J]. : , 2016, 46(8):939-968

[31] , , . [J]. , 2016, 22(1):10-13+18

[32] , , .
[J]. , 2013, 11(11):106-109

[33] p β6

AspenPlus

1 2 1 2

1. 611731 2. 611731

AspenPlus

/

CO H_2

ER / ER 0.35 / CO

AspenPlus

X703 A 1001-9006 2022 02-0021-07

Simulation of Plasma Gasification of Refuse Derived Fuel and Paint Waste Based on AspenPlus

XIE Fei[1], *XU Yinglu*[2], *HU Chunyun*[1], *WU Jiahua*[2]

1. Dongfang Electric Clean Energy Technology Chengdu Co.,Ltd., 611731, Chengdu, China;

2. DEC Academy of Scince and Technology Co.,Ltd., 611731, Chengdu, China

Abstract: In this paper, the plasma gasification model is established by using Aspenplus software. Aiming at different mixing ratios of refuse derived fuel and paint waste , the different plasma input power, air addition and water vapor / air addition on the characteristics of syngas are studied. The results show that the increase of plasma input power is conducive to the increase of calorific value of gasification syngas. With the increase of the proportion of paint waste , the component contents of CO and H2 in syngas can be changed, which is conducive to the further utilization of syngas. ER and steam / air ratio are important factors affecting the gasification process. When ER is 0.35, the gas production rate of syngas is the highest. When the steam / air ratio increases, the CO content decreases gradually. Therefore, the type and dosage of gasification agent should be controlled according to the specific utilization mode of syngas.

Keywords: plasma gasification AspenPlus simulation refuse dezi

غ

EPJ قمم [4] .

CO

غ

ضي ١ أ .

غج ضي

غج ١ [5]

ASPEN

PLUS قمم O_2 غ CO_2

غ أ ڀ .

غج ذ

O_2 . CO H_2 غ

72% . CO H_2 غ

82.1% CO_2 . CO H_2 غ

82.4% . H_2O غ CO_2

. CO غ H_2

.

O2 ∪

1.614 m^3/kg غ CO_2

[6]

AspenPlus جي عمه

.

.

.

ضي . أ

جي عمه

غج أ أ

AspenPlus .

1

1.1

AspenPlus نه .

أ . ١ .

جي عمه

ضي

/ ذ .

. .

نه .

أ ضي . أ أ

كح أ .

أ ١ غ ١ أ ١ ڀ أ

١ ~شخ أ ١

أ . ă

كح أ ~ كح

أ ١ HTZ أ ١ LTZ

H_2O CO CO_2 CH_4 N_2 O_2 C S COS SO_2 H_2S ضي AspenPlus

قمم RK-Soave

FEED1 قمم HCOALGED غ

قمم DCOALLIGT ASH

يح قمم أ

1 شجـ ڀ يح قمم 1

1 AspenPlus

شجـO	Aspen Plus قمم شجـ	
HX0	HEATER	كح
HX3	HEATER	
DECOMP	RYIELD	كح أ
HTZ	RGIBBS	١ أ . كح أ
LTZ	RGIBBS	١ أ . كح أ
B1	RSTOIC	أ . كح أ
SEP1	SEP	
SEP2	SEP	أ كح
SEP3	SEP	
MIX	MIXER	كح
MIXO2	MIXER	كح .

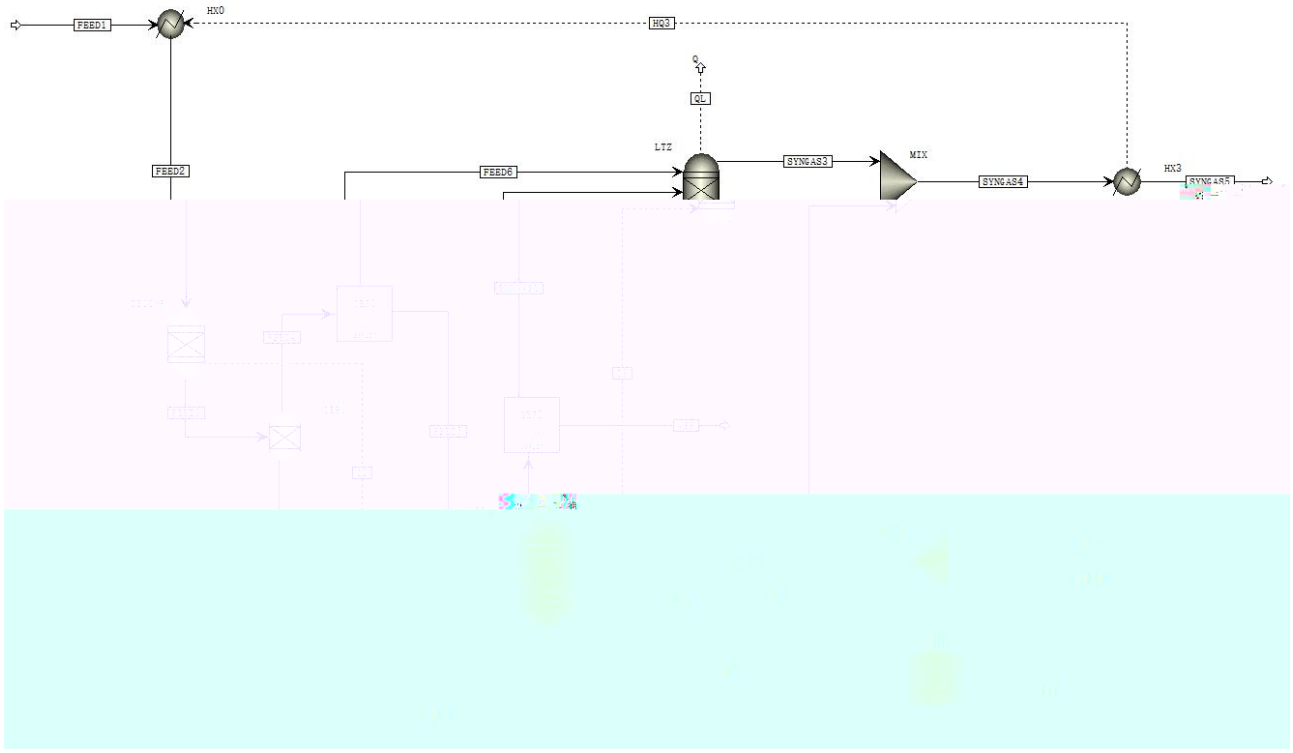

1

1.2

ةمم ٨ جي ئمه جي ئمه ٨

أ ٨ 2

2

	/%			/(kJ/kg)		/%			
	ں	ھ		C	H	O	N	S	
جي ئمه	6.65	71.64	9.98	11.73	21.97	48.73	6.54	26.95	0.85	0.29

٨ 3

3

CO	0.221 3	0.227 7
H_2	0.159 1	0.151 3
CO_2	0.094 8	0.099 8
N_2	0.399 8	0.4
H_2O	0.124 2	0.120 6
SO_2	0.000 7	0.000 6

3 ةمم

جي ﷺ

20% 1.16 Nm^3/kg

C H CO

H_2 . CO H_2

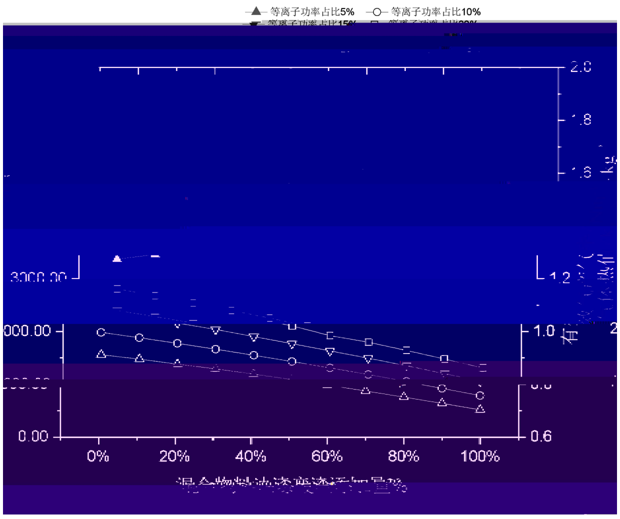

2

2 3

CO H_2

2 3

ER

ER

H_2 ↄ

H_2

Ь U *S/A*

H_2 ڏ

ↄ

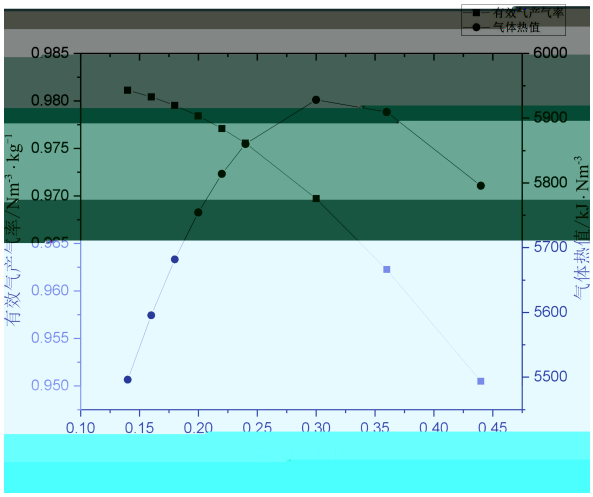

6 /

□ *S/A* ڏ ۓ

7 ۓ 7 *S/A* CO ↄ

8.28% 2.21% H_2 ↄ 26.77%

27.86% U 26.73% غ

ĭ h H_2 غ CO_2 ↄ

CO ↄ ۷

H_2 CO

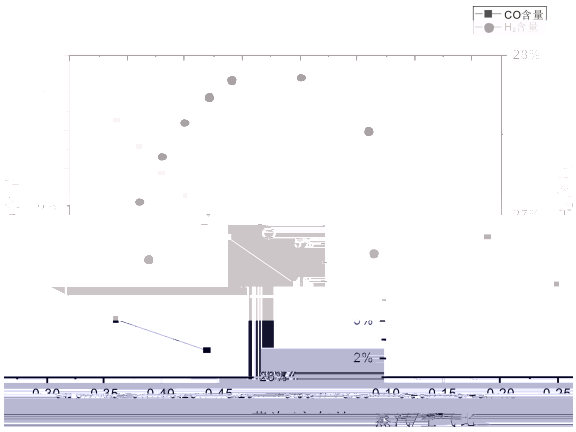

7 /

3

1 ججي .

۱ .

ĭ H_2 CO غ H_2 ↄ

. ضي

2 / ڏ .

غج / أ

أ.

CH^4 ↄ ĭ غج

ĭ h . ĭ

/ ڏ CO H_2 ↄ

/ CO ↄ غج

/

أ ↄ

3

Ь U

4 / ڏ Ь U

5 □ .

. غ

. غ

---

[1] . غج ججي ضي [J]. غ , 2002, 3(3):65-68

[2] ۷. ججي [D]. : , 2009

[3] , , . غج ججي . [J]. . , 2012, 32(12):20-24

[4] MOUNTOURIS A, VOUTSAS E, TASSIOS D. Solid waste plasma gasification: equilibrium model development and energy analysis[J]. Energy Conversion and Management, 2006, 47(13-14):1723-1737

[5] . ĭ ۱ . ۱ ۷ .2005

[6] , , ŭu . ASPEN PLUS ججي . [J]. . 2014,36(2):1-5

P Fe_3O_4

510620

HER

HER HER

Fe_2O_3

P Fe_2O_3 Fe_3O_4@P

Fe_3O_4@P Fe_2O_3

Fe_3O_4 P

TQ426 A 1001-9006 2022 02-0028-05

Preparation of P-doped Fe_3O_4 Nanoarrays for Boosting Hydrogen Evolution Performance

PAN Jun, *LU Yanshan*, *HUANG Xurui*, *ZHANG Hang*, *HE Binbin*

(Guangzhou Power Supply Bureau, Guangdong Power Grid Co., Ltd.,510620,Guangzhou,China)

Abstract: Because most of the traditional electrocatalytic hydrogen evolution reaction (HER) catalysts are precious metal catalysts, which can not be widely used, the development of non precious metal catalysts that can be popularized is a breakthrough in the field of HER. As the most abundant transition metal element in nature, iron oxide has been proved to have certain catalytic performance in HER. Based on foam iron, Fe_2O_3 nano sheet array was prepared by anodic oxidation method to increase its surface area and increase catalytic active sites. Then P was doped into the material in a vacuum tube furnace to improve its catalytic performance, and finally Fe_2O_3 nano chip array was transformed into Fe_3O_4@P nano chip array. Through morphology characterization and electrochemical test, the material shows certain catalytic performance, and the performance of the modified material Fe_3O_4@P nano chip array is obviously better than Fe_2O_3 nano chip array.

Keywords: electrocatalytic hydrogen evolution; anodic oxidation; Fe_3O_4; nano chip array; P doping

2022-01-19

GZHKJXM20200090

1981 2006

[1-2]

HER

Pt, Ru

[3-4]

HER

Mo Co Ni Fe

[5-9]

Fe

-

Fe P

(TMPs)

[10-12]

[13-15]

P

P

P

Fe_2O_3 Fe_3O_4

1

1.1 Fe_3O_4

Fe_2O_3

0.5 wt% + 3 vol% +

2.5 cm

1

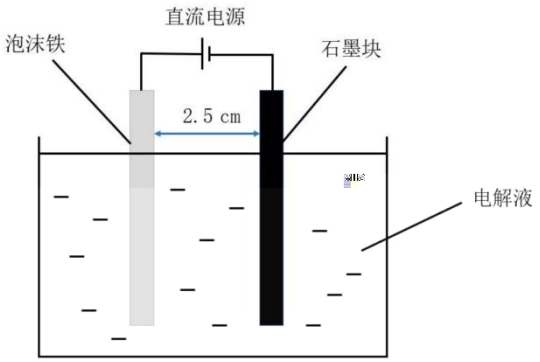

1

1

50 V 5 min

4h

Fe_2O_3 NaH_2PO_2

1:5

2

P

P NaH_2PO_2

Fe_2O_3

P

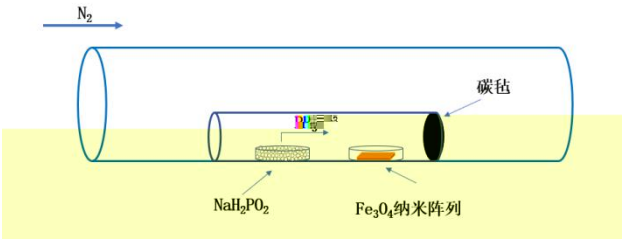

2 P

NaH_2PO_2

PH_3 PH_3 P H_2

NaH_2PO_2 PH_3

PH_3

PH_3 PH_3 P

H_2 Fe_2O_3 P Fe_3O_4

$$2NaH_2PO_2 ==== Na_2HPO_4 + PH_3$$

$$2PH_3 ==== 2P + 3H_2$$

$$3Fe_2O_3 + H_2 ==== 2Fe_3O_4 + H_2O$$

KOH

15

2 /min 350

2 h

P Fe_3O_4

1.2

XRD Rigaku D/max 2500

PC X Fe_2O_3

P Fe_3O_4@P

Cu Kα λ=1.540 6 Å

40 kV 20 mA 4°/min

5~85° ZEISS Gemini

300 Fe_2O_3

P Fe_3O_4@P

CHI660E

P Fe_3O_4 1 ×

1cm

Hg/HgO

50 mL 1.0 mol/L

30 min

Hg/HgO

LSV LSV Tafel

EIS

- I-t

2

2.1 XRD

3 Fe_2O_3 Fe_3O_4@P

XRD

45.37° 65.72° 82.91°

3 a XRD 29.71° 34.85°

43.23° 53.92° 62.90° Fe_2O_3

112 211 220 024 224

3 b XRD 32.45° 37.24°

38.35° 44.34° 56.83° 63.41° Fe_3O_4

220 311 222 400 511 440

P

XRD Fe_2O_3 Fe_3O_4

Fe_2O_3 Fe_3O_4

P

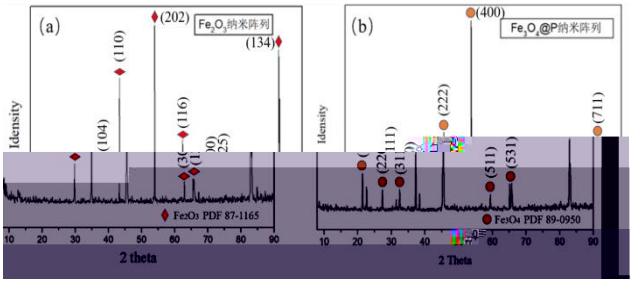

a Fe_2O_3 b Fe_3O_4@P

3 XRD

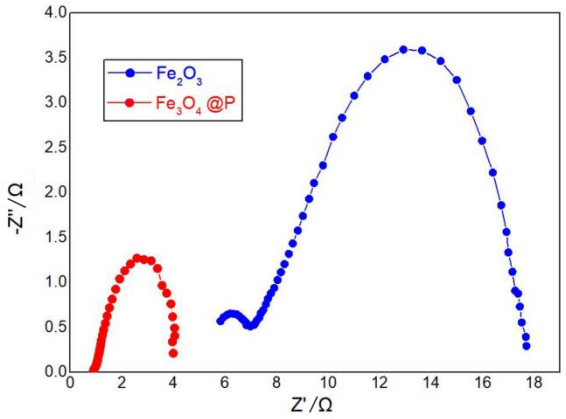

8 Fe_2O_3 Fe_3O_4@P EIS

10 mV/cm^2

9 Fe_2O_3

Fe_3O_4@P

Fe_3O_4@P

Fe_2O_3 P

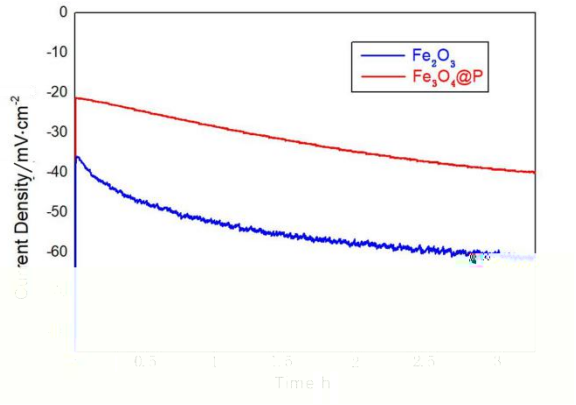

9 Fe_2O_3 Fe_3O_4@P I-t

3

Fe_2O_3 Fe_3O_4 P

Fe_3O_4@P Fe_2O_3

[1] CHEN Y, RONG J, TAO Q, et al. Modifying microscopic structures of MoS2 by high pressure and high temperature used in hydrogen evolution reaction [J]. Electrochimica Acta, 2020, 357:136868

[2] MUGHERI A Q, ALI S, NAREJO G S, et al. Electrospun fibrous active bimetallic electrocatalyst for hydrogen evolution [J]. International Journal of Hydrogen Energy, 2020, 45(41): 21502-21511

[3] GUO Z, LI W, HE Y, et al. Effect of Cd source on photocatalytic H2 evolution over CdS/MoS2 composites synthesised via a one-pot hydrothermal strategy [J]. Applied Surface Science, 2020, 512:145750

[4] CAI Y, KANG H, JIANG F, et al. The construction of hierarchical PEDOT@MoS2 nanocomposite for high-performance sun@(

Fe_2O_3

1 2 1 1 1 1

1. 614200 2. 611731

80

80 g/L 2 h 1.3 1.5

1.6 93% 95%

X705; TQ125.3 A 1001-9006 2022 02-0033-04

Study on Recovery Technology of Tellurium and Cadmium from Cadmium Telluride Waste

LEI Cong[1], *YUAN Xiaowu*[2], *ZHANG Cheng*[1], *YANG Wuyong*[1], *LEI Yundi*[1], *JIANG Jiechang*[1]

(1.Emei Semiconductor Material Institute, 614200, Emeishan, Sichuan, China;

2.DEC Academy of Science and Technology Co., Ltd., 611731, Chengdu, China)

Abstract: The recycling process of tellurium and cadmium from cadmium telluride waste was studied by grinding, oxidation acid leaching, reduction reaction etc. The results show that the acid leaching temperature is 80 , the sulfuric acid concentration is 80g / L, the acid leaching time is 2h, the mass ratio of material to hydrogen peroxide is 1.3, the mass ratio of sodium sulfite to material is 1.5, and the mass ratio of sodium sulfide to material is 1.6. Under these conditions, the recycling of tellurium and cadmium is more than 93% and 95%.

Keywords: cadmium telluride; oxidizing acid leaching; reduction reaction; rate of recycling

CdTe 240

-

γ

[1]

Te “

”

[2-4]

Cd

1

1.1

1.2

2021-11-18

1984 2007

99.999%

1

1

	Te	Cd	
	53.16%	46.83%	0.001%

1.3

$CdSO_4$ H_2TeO_3 Na_2SO_3

$CdSO_4$

[4-5]

$$CdTe + H_2SO_4 + 3H_2O_2 \rightarrow CdSO_4 + H_2TeO_3 + 3H_2O \quad (1)$$

$$Na_2SO_3 + H_2SO_4 \rightarrow Na_2SO_4 + H_2O + SO_2\uparrow \quad (2)$$

$$SO_2 + H_20 \rightarrow H_2SO_3 \quad (3)$$

$$H_2TeO_3 + 2H_2SO_3 \rightarrow Te\downarrow + 2H_2SO_4 + H_2O \quad (4)$$

$$Na_2S + H_2SO_4 \rightarrow Na_2SO_4 + H_2S\uparrow \quad (5)$$

$$CdSO_4 + H_2S \rightarrow CdS\downarrow + H_2SO_4 \quad (6)$$

1.4

98% AR H_2O_2 30%

Na_2SO_3 AR Na_2S AR

ICP-MS

PH PH

(3000 mL×2 500 mL×2 100 mL×2 250 mL×1 100 mL×1 50 mL×1

(500 mL×3 500 mL×2

10 mL×10 5 mL×10

1.5

0.2 mm

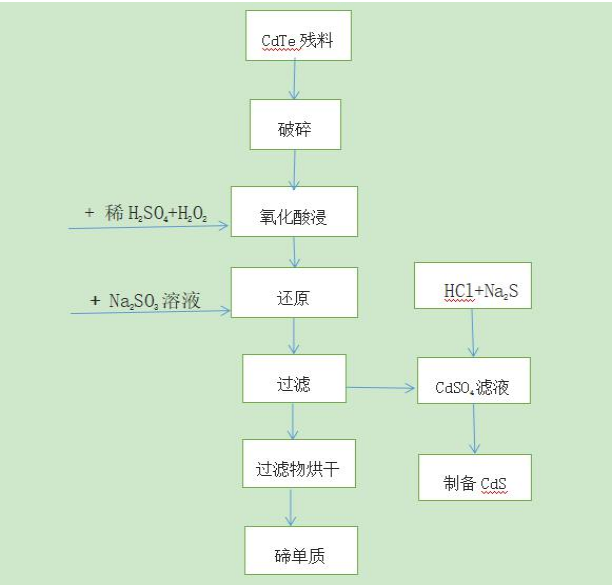

1

2

2

80

93% 80

2.2

0.2 mm

H_2SO_4 1: 6

80 2h 30%

/ 1.3 Na_2SO_3

1.5 Na_2SO_3 /

Na_2S 2.4 Na_2S /

3

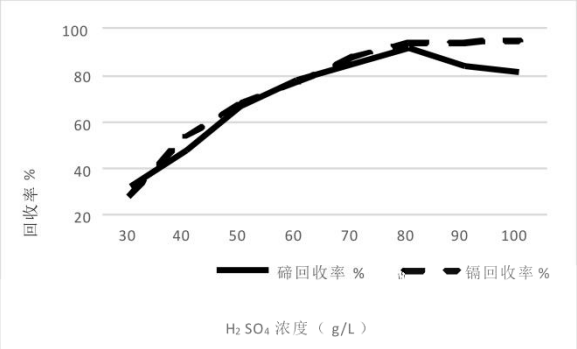

3 H_2SO_4

3

30 g/L

80g/L 30%

92% 90 g/L

80g/L

2.3

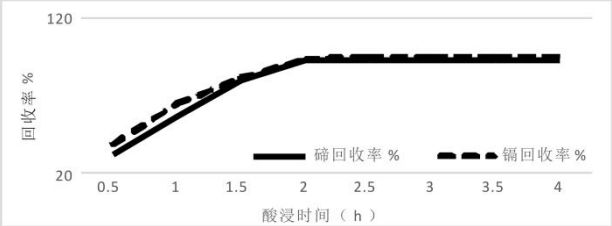

4

0.2mm

H_2SO_4 80g/L H_2SO_4

1:6 80 30%

/ 1.3

Na_2SO_3 1.5 Na_2SO_3 /

Na_2S 2.4 Na_2S /

4

4

0.5

2 30%

94% 2

2

2.4

0.2 mm

H_2SO_4 80 g/L H_2SO_4

1: 6 80 2h

Na_2SO_3 1.5 Na_2SO_3 /

/

5

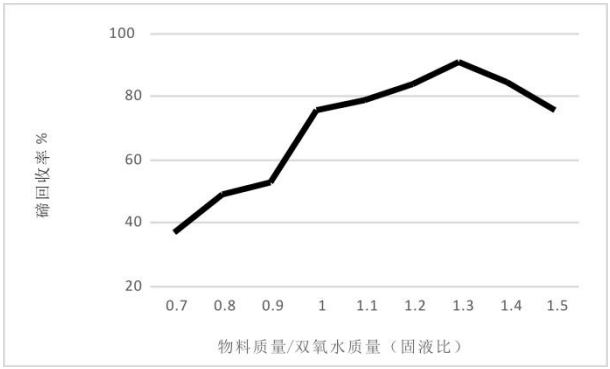

5

5

0.7 1.3

37% 92%

1.3

2.5 Na_2SO_3

H_2TeO_3 $CdSO_4$

Na_2SO_3 H_2TeO_3

Na_2SO_3

6

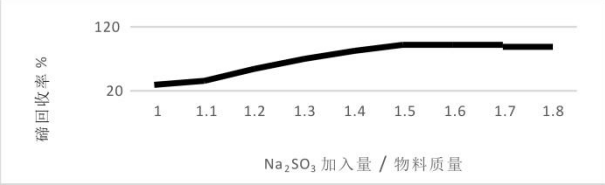

6 Na_2SO_3

6

H_2TeO_3 Na_2SO_3

Na_2SO_3

1 1.5 28% 93%

Na_2SO_3

Na 2

Na_2SO_3

1.5

2 Na

Na_2SO_3	Na ppm
1.5	132
1.6	435
1.7	1 342
1.8	5 428

2.6 Na_2S

$CdSO_4$

Na_2S

Cd^{2+} Na_2S

7

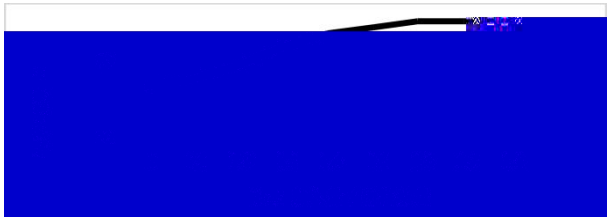

7 Na_2S

7

$CdSO_4$ Na_2S

Na_2S ς

430223

X

TL353.13 A 1001-9006(2022)02-0037-04

The Study of Material Performance and Residual Stress Changes on RVI Core Barrel after Local Deformation

XIAO Shuixian, *ZHOU Yingping*, *DONG Mingliang*, *SHU Huaan*

(Dongfang Electric (Wuhan) Nuclear Equipment Co., Ltd., 420223 Wuhan, China)

Abstract: Austenitic stainless steel is the main material of the RVI in light water reactors. As an important part of RVI, core barrel has stringent requirement of dimensional accuracy. After welding, the local core barrel is usually required to be circle checked. In that processing, improper operation may cause local deformation, which can change the properties of the materials, the residual stress distribution will also be changed. This paper researched regulation of local deformation, dimensional stability heat treatment affecting on material performance and residual stress, by material mechanics experiment on simulator of local deformation, and stress measurement on the surface of core barrel in different stages.

Key words: barrel austenitic stainless steel local deformation material performance residual stress

[1]

X

2022-04-20

1987 2010

1

1.1

Z2CN19-10+N_2

1

1 Z2CN19-10+N2

wt%

C	Cr	Ni	Si	Mn	S
≤0.035	18.50 20.00	9.00 10.00	≤1.00	≤2.00	≤0.015
P	Cu	B	N	Co	
≤0.030	≤1.00	≤0.0018	≤0.080	≤0.06	

1.2

52 mm D3400 mm

1 m

20 mm

31 mm 400 mm

1

19 mm 34 mm

2

400 ×8h

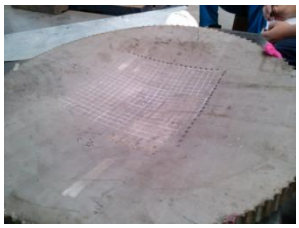

1 2

1.3

1.3.1

4

1

2

3

4

3 4 RCC-M M3310(2000 +2002)

1.3.2

1

5

4

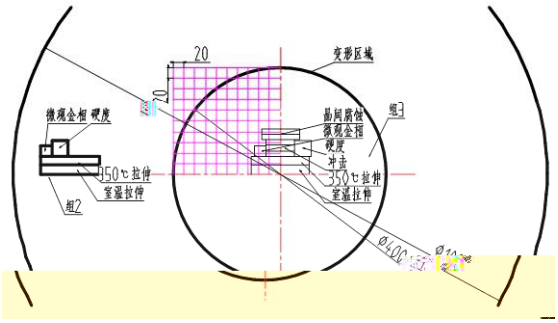

3

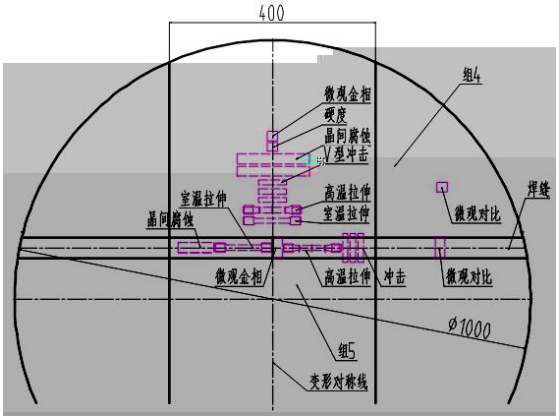

4

1.4

1.4.1 2

2

	350						
	$Rp_{0.2}$/MPa	Rm/MPa	A/%	$Rp_{0.2}$/MPa	Rm/MPa	/J	/HB
	≥210	≥520	≥40	≥125	≥394	≥60	/
1	248	563	62.5	133	417	272,274,277	/
	261	576	60.0	132	412	293,271,274	/
2	325	575	58.5	235	430	/	180
	275	575	59.5	185	435	/	172
3	350	566	59	266	433	317,323,341	216
	447	616	48.5	367	464	297,300,309	228
4	301	587	59	213	435	353,349,352	235
	309	606	57.5	213	440	333,411,365	225

2

(1) 350

(2) 350

(3)

1.4.2 , 3

3

	350					
	Rp0.2/MPa	Rm/MPa	A/%	Rp0.2/MPa	Rm/MPa	/J
	≥ 210	520~700	≥ 30	≥ 125		≥ 60
	510	630	43.5	430	480	210,238,233, 200,209,232
	416	594	41.5	364	441	191,175,179
5	490	593	47.5	367	422	211,187,225

3

1.4.3

3 4 5

RCC-M MC1310

B

1.4.3

3 4 5

2

2.1

[2]

[3]

2.2

X JV iXRD

2dsinθ=nλ

X

X

Δθ

Δd

X

5 30 μm Mn

10 μm

2.3

4

1

2

3

5

4

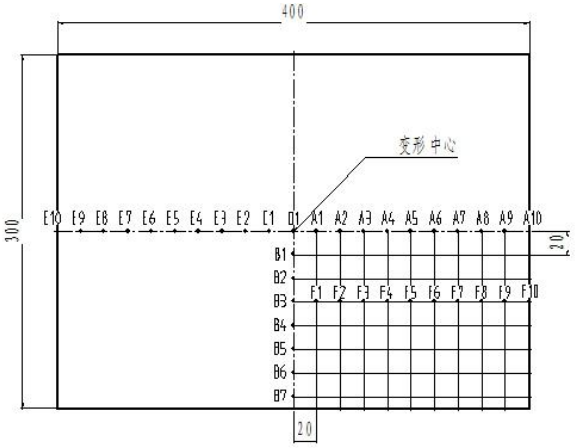

5

2.4

1 2 4 4

4 1 2 4

MPa

	1	2	3	4	5
1	516	505	502	516	574
1	-327	-198	-349	-387	-388
2	-617	-579	-570	-	-
4	477	-	-	-	-

3 5

5 3

MPa

	1	2	3	4	5	6	7	8	9	10
O	-459	-	-	-	-	-	-	-	-	-
A	-450	-15	-151	-509	80	225	-217	493	-123	-25
B	-404	-367	-368	-313	-309			-	-	-
E	-488	-400	11	328	467	195	117	-39	231	187
F	-353	-268	-354	-466	-652	-592	-658	-615	-636	

2.5

4 1

2

[4] 2

5

[5]

30kPa 6

MPa

(

)

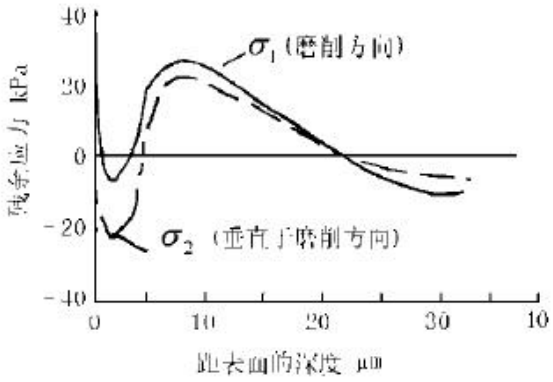

6

5 493 MPa,

20%

620

MPa 574

MPa

476 MPa

493 MPa

3

20 mm 30 mm

400 mm X

(1) 350

350

(2)

(3)

(4)

下 56

ER316H

511455

ER316H

ER316H

ER316H

TG441.8 A 1001-9006 2022 02-0041-03

Research on Influence of Heat Treatment Process on Mechanical Properties of ER316H Deposited Metal

JIANG Yuchen, LI En, HE Bing, ZHANG Danping

(Dongfang Electric (Guangzhou) Heavy Machinery Co.,Ltd., 511455, Guangzhou, China)

Abstract:In this paper, focusing on ER316H argon arc welding wire of stainless steel welding wire for nuclear island equipment, through welding process tests under different heat treatment systems, the influence of different heat treatment holding time on high temperature tensile strength, room temperature impact performance of ER316H deposited metal is obtained. A foundation has been made for the research and use of stainless steel welding materials for steam generators in related projects.

Key words: ER316H; Argon arc welding wire of stainless steel; heat treatment holding time; tensile strength; impact energy

ER316H

2022-04-20

1991 2015

第36卷Vol.36总第142期

1 5# 6# 7#

1

ER316H TIG

7-20 L/mn

690 ±15

ER316H

2

AWS B4.0M-2000 ASTM E21-1998

1# 2# 3# 4#

ER316H

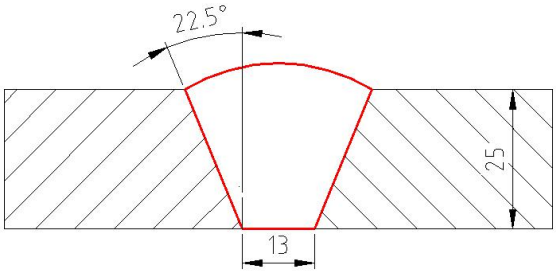

1

1 ER316H

wt%

	C	S	Si	Mn	P	Cr	Ni	Mo	Cu	Co	Pb
ER316H	0.51	0.001	0.47	1.61	0.005	18.48	12.76	2.35	0.02	0.01	0.001

Sn	**As**	**Sb**	**Bi**	**Al**	**V**	**Nb**	**N**	**B**	**Ca**

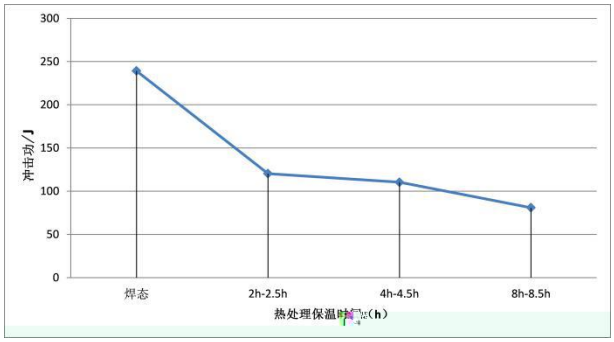

3

TIG

248 J

8 h-8.5 h

86 J 65%

[2] 4

a

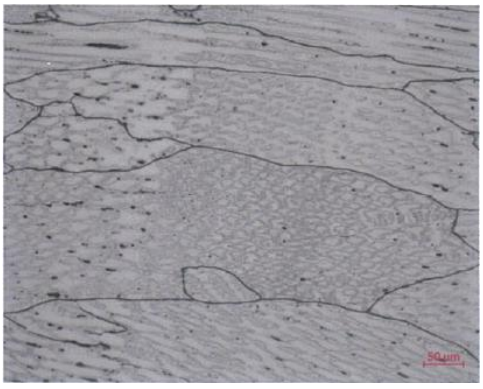

b

4

ER316H

5# 6# 7# 750 /100h

1 5

1 5

5

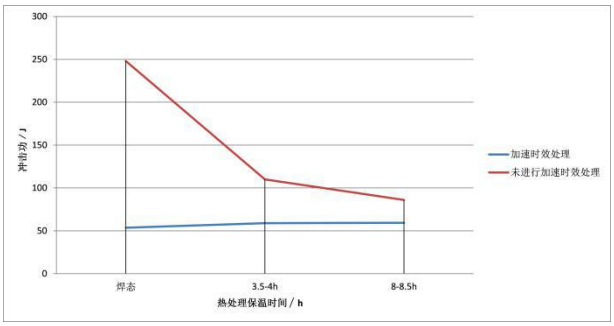

5

750 /100h

σ [3]

6

6

2.3

AWS B4.0M

4

180°

下 60

1,2

1. 611731 2. 643001

660 MW

TK223 A 1001-9006 2022 02-0044-06

Research and Application of Steel Structure Optimization for Large Capacity Boiler

GAO Ling[1,2]

1. Clean Combustion and Flue Gas Purification Key Laboratory of Sichuan Province, 611731, Chengdu, China;

2. Dongfang Boiler Group Co.,Ltd., 643001, Zigong, SiChuan, China

Absrtact: With the increasingly fierce market competition, the cost control requirements of products are more and more strict. As the steel structure supporting the suspended boiler, how to achieve both safety and economy is a problem that all structural designers must consider. Taking the steel structure of 660MW high efficiency ultra supercritical boiler as an example, the optimization design of steel structure is systematically considered and studied.

Key words: steel structure; optimization research

1

1

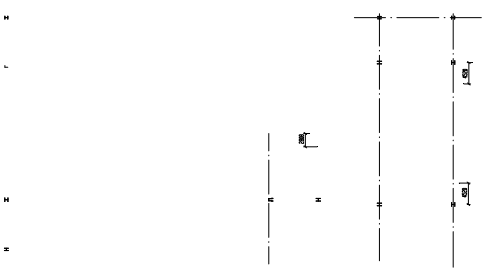

2022-04-20

1982 2005

2 3

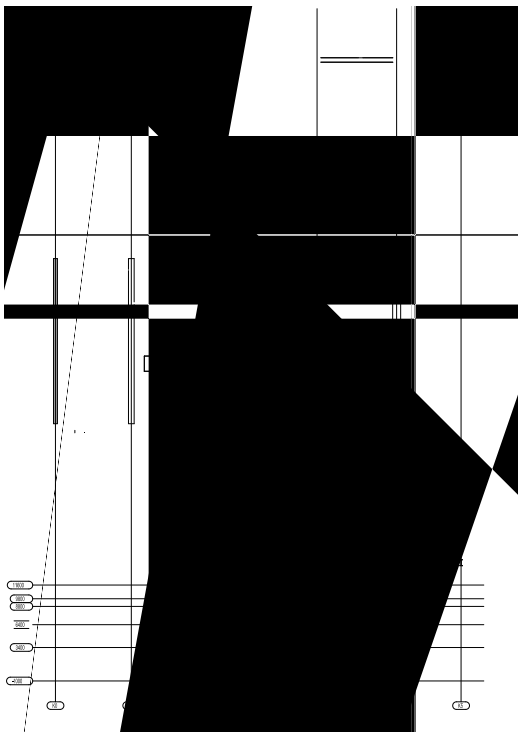

8

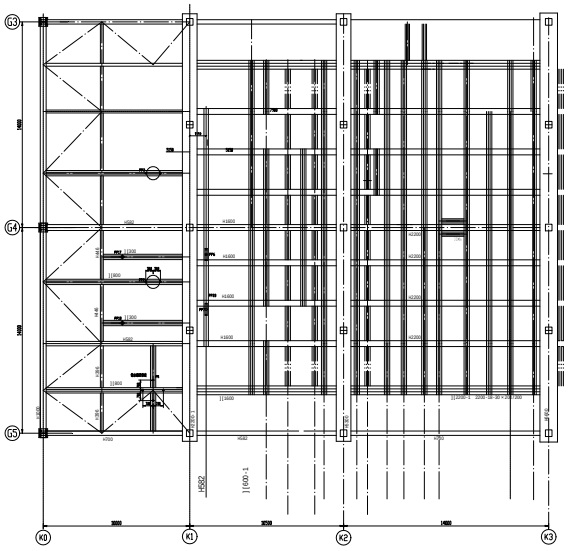

5.1.1

50 m

50 m

0 m

50 m

2

11

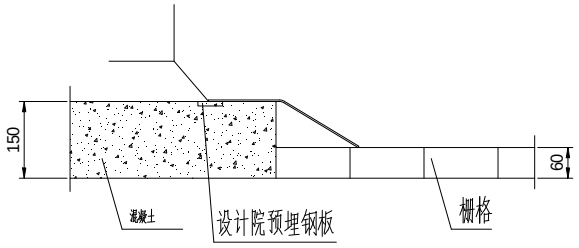

4.3

“ ”

1

10

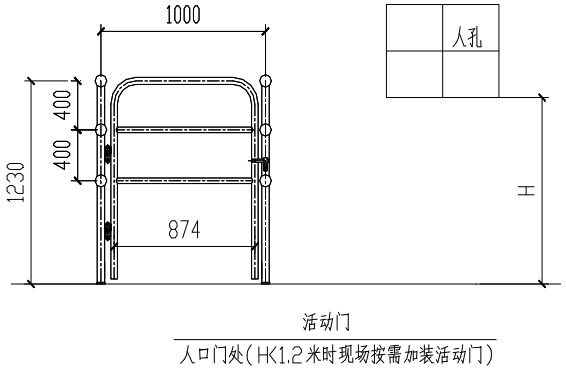

10

“ 2025 ”

[8]

70%-80%

1

4

[9]

(1)

(2)

(3) (MOM)

(4)

2

2.1

2.1.1 (VPI)

2.4 kV/mm~3.2 kV/mm

2.1.2

[10] /

[11]

(1) WBS

24

(Automated Guided Vehicle AGV) 2 3

1

1 1 1

40 ;

60 ;

40 AGV 4

3

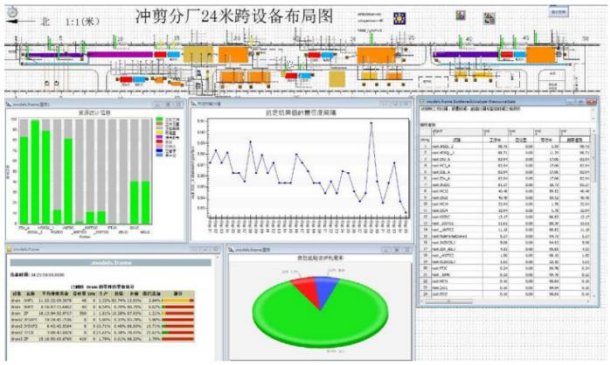

1

(2)

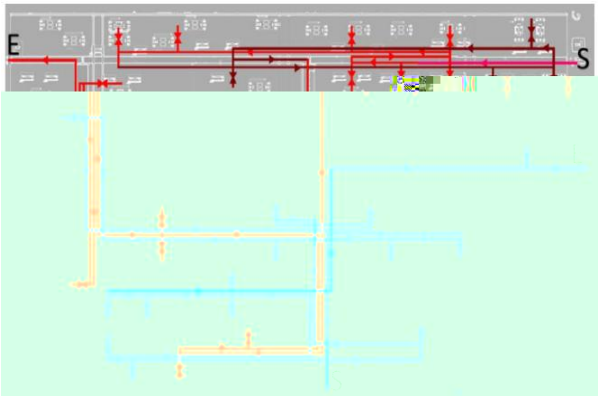

2

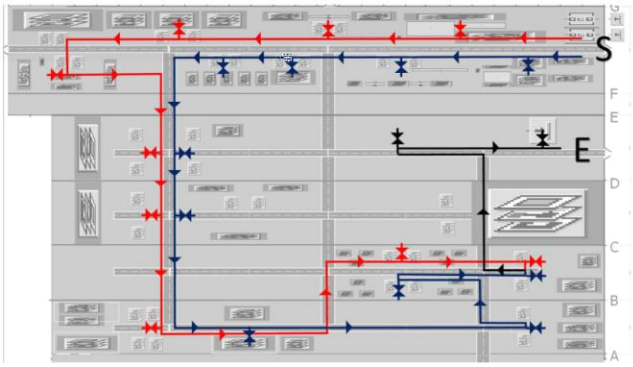

3

2.1.3

1:1

( )

( ) [12] PostEngineer

4 5

2.2

( )

4

5

2.2.1

(1)

(2)

9 12

;

(3)

50%~72%

3~4 98%

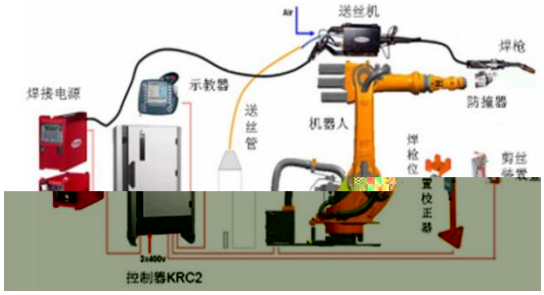

6

2.2.2 AGV

400t

(1)

PLC ;

AGV

(2) Hymmen Hymmen

(3)

(4)

AGV

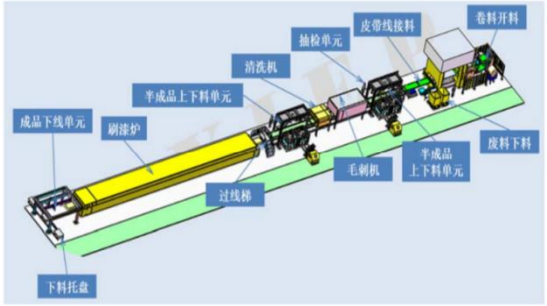

7

2.2.3

3D

0.1

2.3

2.3.1

PDA

[13]

DM

(3)

[14]

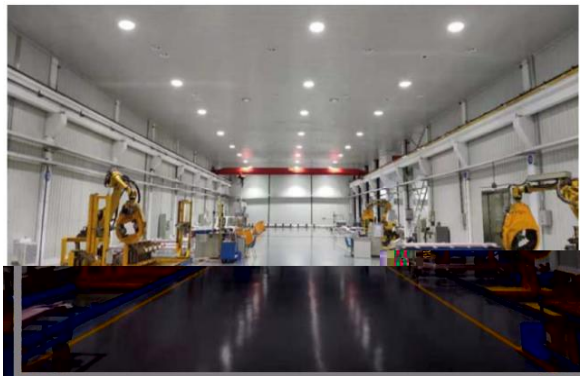

MOM

2.3.4

11

80

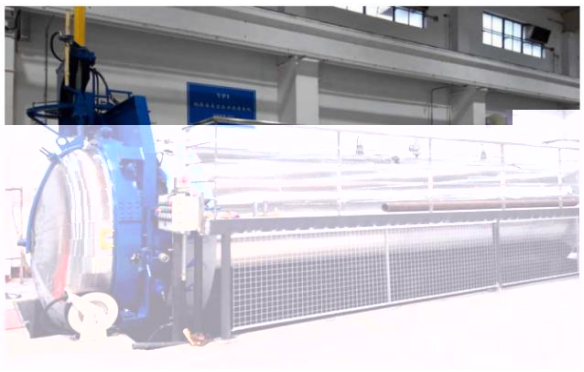

12 VPI

MOM

(1)

LED

VRM

7 m

0.1 mm 4

15

[15]

MOM MOM

3

(2)

APP PDA ,

APP

WIFI MOM PDA

;

600 MW

18 14

48.2% 31.9%

30.7% 20%

57.3%

28%

21.3% 54.8%

VPI

25%

45%

35% 55%

33.5%

[1] ANNUNZIATA M EVANS P. Ilndustrial lnternet: pushing the boundaries of minds and machines[J]. General Electric 2012(1-2): 1-23

[2] KAGERMANH HELBIG J HELLINGERA et al. Recommendations for lmplementing the strategic niative NDUSTRIE 4.0:Securing the future of German manufacturing industry ; final report of the Industrie 4.0 working group[M]. Berlin:Forschungsunion 2013

[3] 2025[EB/OL]. [2015-05-08]. http:/lwww.gov.cn /zhengcelcontent/2015/05/19/content_9784.htm

[4] , , . ——[J]. 2017, 23(1):1-9

[5] , , , , . [J]. 2016 22(5):1220-1228

[6] . i5 [J]. 2017 46(1):1-8

[7] , . [J]. 2018 54(16):11-23

[8] . 4.0[J]. 2015(25):1-3

[9] —— [J]. 2016(9) : 1-5

[10] . [J]. , 2018(4) : 10-15

[11] . 4.0 [J]. , 2018(15) : 65-66

[12] , , . [J]. , 2017(24) : 9-12

[13] . [J]. 2017(9): 28-35

[14] , , . [J]. ( ), 2017(2):128-133 +140

[15] , . [J]. , 2016(9):2108-2117

上 40

5

4

[1] , , . [J]. , 2011, 32(10):813-816

[2] , . [J]. , 2011, 28(1):11-15+41

[3] , , . sss [J]. , 2007, 228(6):213-216+220

[4] , . sss [J]. , 2010, 10(21):5145-5150

[5] , . sss [J]. , 2007, 234(8):101-103

261400

TM62 A 1001-9006 2022 02-0057-04

Research on Test Method of Online Monitoring and Analysis Software for Generators in Smart Power Plant Based on Expert Simulation Fault Data

WANG Chuangang, *ZHAO Yanan*

(Huadian Laizhou Power Company Co., Ltd., 261400,Laizhou, Shandong, China)

Abstract:Intelligent diagnostic software is an important part of "smart power plant". This paper proposes an intelligent diagnosis software test method based on expert simulation fault data, and builds a set of generator online monitoring and analysis software test platform. The intelligent diagnostic software testing method is based on expert knowledge, combined with the real operating data, typical fault data and generator operation and maintenance fault database of the same model generator set to construct expert simulation fault data and fault list. The expert simulation fault data is input into the generator online monitoring and analysis software for diagnosis, and the diagnosis result is obtained. By comparing the diagnosis result with the expert simulation fault list, the

1

1

1

1	
2	aServer-R-2105 V6.0
3	V6.0 V3.0
4	1000MW
5	Cloudera’s Distribution Including Apache Hadoop(CDH)
6	Kubernetes(k8s)
7	
8	
9	M420

2

1

aServer-R-2105

V6.0

V6.0 V3.0

CDH

k8s CDH

[3]

k8s

1

1 000 MW

web

3

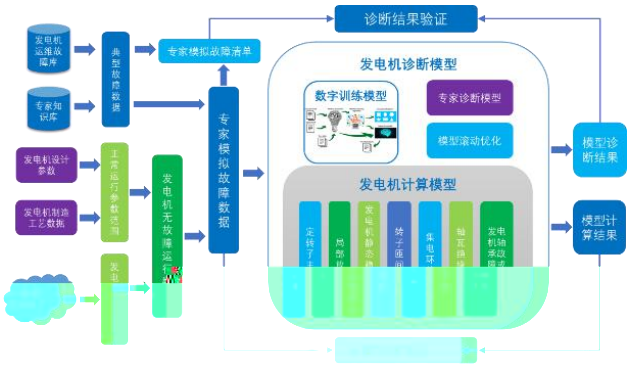

2

2

3.1

1 000 MW

——

n1

n2

1 000 MW n3 n3

≤ n2 n3 ≤ n1

7 n2 ≤ n1

$$= \frac{n2}{n1} \times 100\% \quad (1)$$

$$= \frac{n3}{n1} \times 100\% \quad (2)$$

n2 n1

$$= \frac{n1}{n2} \times 100\% \quad (3)$$

$$= \frac{n3}{n2} \times 100\% \quad (4)$$

95%

90%

3.2

4

100 kW

30

95% 50

3.3 30

5

80

5

5

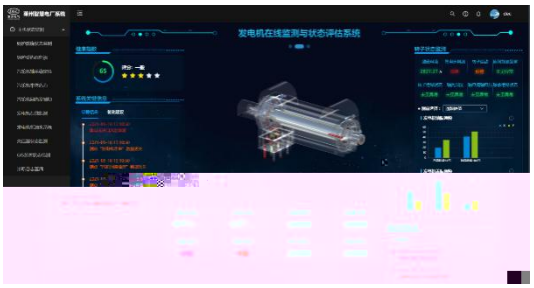

3

3 web

3

3

1	30	1 000	962	931	96.2%	93.1%
2	30	1 000	953	927	95.3%	92.7%
3	30	1 000	957	924	95.7%	92.4%

5

[1] , , . [J]. , 2019, 48(10): 8-14

[2] . [D]. : ( ), 2018:3-4

[3] . Storm Kafka [J]. ,2021,34(5): 33-34+36

[4] , , . [J]. , 2021, 51(3): 1017-1025

上 43

GB/T 4334 “ E ”

3

+ +

650 ×2 h

3

ER316H

690 ±15

1 ER316H

2 ER316H

3 ER316H

[1] . [J]. , 2011(35):91

[2] , , . 800MPa [J]. , 202

611731

TM621 A 1001-9006 2022 02-0061-04

Analysis of Typical Medium Speed Milling System Retrofit for Peak Load Regulation

WEI Lijun, *NING Xiaorui*, *ZHANG Yupeng*

(Dongfang Electric(Chengdu) Engineering & Consulting Co.,Ltd., 611731,Chengdu, China)

Abstract: With the goal of carbon peak and carbon neutralization, the domestic power supply structure of China needs to be adjusted to consume more green power. Traditional thermal power units are facing the pressure of retrofit to meet the demand of deep peak regulation. In this paper, based on the flexible operation retrofit of one thermal power plant, we carried out the theoretical calculation of low load operation condition of medium speed mill, and compared with the commissioning operation result, in order to provide reference for the evaluation and retrofit of similar pulverizing system to meet the low load operation demand of boiler.

Keywords: peak load regulation; flexibility; direct firing pulverizing system; medium speed milling

2021 ”

10 2030

35% ,

6 h

40% “

[1] ” 2

2021 1519 “

2022-04-01

1983 2008

“ ”

2016 1

25%THA

[2]

1

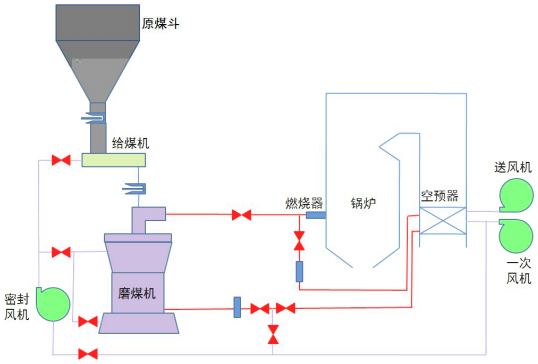

1

HP MPS ZGM

MPS-HP- E

MPS170-HP- MPS

[3]

1

2 × 330 MW

DG 1025/18.2- 6

π 2016 7

-

1

1

				1	2
	M_{ar}	%	5.5	17	17
	A_{ar}	%	28.19	25	28
	C_{ar}	%	52.67	47.01	43.5
	H_{ar}	%	3.22	3.21	3.21
	O_{ar}	%	8.43	5.53	6.04
	N_{ar}	%	0.75	0.75	0.75
	$S_{t,ar}$	%	1.34	1.5	1.5
	V_{daf}	%	31.38	34	35
	$Q_{net,ar}$	kJ/kg	20 223	18 280	17 080
	HGI	/	76.0	55	55

1

4

2

2

-	
-	MPS170HP—
-	SLK310 ( )
	5
t/h	43.58
t/h	60.58
Pa	6160
rpm	34.45
	≤90
-	
t/h	0.072
-	
-	YMPS450—6
kW	355
A	49.4

R_{90} 22% 4

BMCR

2

[4]

75%

1

R_{90}

[4]

R_{90}

[5]

R_{90} [6]

R_{90} 12~18%

2

“ ”

“ ”[7]

10%

3

1

3

3

		1
f_H	0.97	0.78
f_R	1.059	1.072 0.944 R_{90}=13%
f_M	0.99	0.91
f_A	0.97	0.95
f_g	1.0	1.0
f_e	0.95	0.95
f_{si}	1.07	1.07
B_M t/h	50.6	38 34.5 R_{90}=13%

HGI B_M

38t/h R_{90}=21% 4

BMCR

R_{90}=13% 34.5t/h 5

R_{90}

2

DL/T 5145

1

100%THA 25%THA

4

4

			100%THA	25%THA
1	Δϑ	kg/kg	0.12	0.12
2	q_{ev}	kJ/kg	316.5	316.5
3	t_2		65	65
4	t_{rc}		0	0
5	q_{ag2}	kJ/kg	108.0	160.0
6	g_1	kg/kg	1.61	2.39
7	c_{a2}	kJ/(kg ·)	1.014	1.014
8	q_f	kJ/kg	72.3	72.3
9	c_{dc}	kJ/(kg ·)	1.101	1.101
10	e	kJ/kg	25	25
11	q_{mac}	kJ/kg	15	15
12	q_s	kJ/kg	0.65	0.71
13	t_1		297.5	228
14	c_{ag1}	kJ/(kg ·)	1.030	1.024
15	d_2	g/kg	86	61
16	t_{dp}		50	44
17		-	1.638	2.50
18	$B_{M,d}$	t/h	30.5	21.1

100%THA 70%
25%THA 2

25%THA

25.23 t/h 21.39 t/h

4

1
R_{90}

2

3

[8]

4 “
”

5 40%~25%THA

SCR

6

[1] . 2021-2022 [DB/OL]. https://cec.org.cn/detail/index.html?3-306171, 2022-01-27

[2] , , . [J]. ,2018,47(5):1-7

[3] , , . MPS-HP- [J]. , 2014,34(9):725-730

[4] DL/T 5145-2012, [S]

[5] , . [M]. : 2010.8

[6] . [J]. , 2014, 35(2):31-33

[7] , , , , . [J]. , 2019,25(2):139-143

[8] . [J]. , 2019(1):1-4+10

1 1 1 2

1. 618000 2. 100022

6.5 4.5

0.8 0.9

TH113 A 1001-9006 2002 02-0065-04

Research on the Bending-torsional Coupling Mode Frequency of Steam Turbine Gear Rotor System

PENG Lin[1], *DONG WeiHong*[1], *ZHANG Jian*[1], *ZHOU Chuanyue*[2]

1.Dongfang Turbine Co.,Ltd., 618000, Deyang, Sichuan, China; 2.Beijing EMAX Technology Co.,Ltd., 100022, Beijing, China)

Abstract This paper established the bending-torsional coupling dynamic model of a complex shaft system composed of a high-pressure steam turbine rotor, a low-pressure steam turbine rotor, a flexible coupling, a high-speed gear rotor, a torsion bar and a quill shaft assembly of a low-speed gear flexible rotor, and a generator rotor. The calculation results show that the bending-torsional coupling effect is significant due to the weak restraint of the gear bearing on the bending vibration of the gear rotor when starting with no load, compared with the calculation results of pure torsion, the first two frequencies of torsional vibration have decreased by 6.5% and 4.5% respectively, so it is necessary to establish a bending-torsional coupling calculation model; during full-load operation, the bending-torsional coupling effect is not obvious due to the strong constraint of the gear bearing on the bending vibration of the gear rotor, compared with the calculation results of pure torsion, the first two frequencies of torsional vibration have decreased by 0.8% and 0.9% resp" ĎT

-

-

API684

[5-6]

1

- -

45 MW 1

5 025 rpm

3 000 rpm

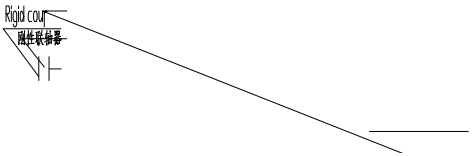

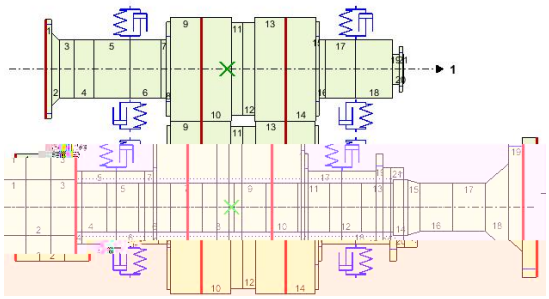

b

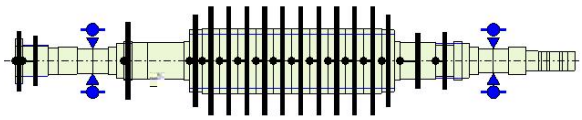

c

3

4

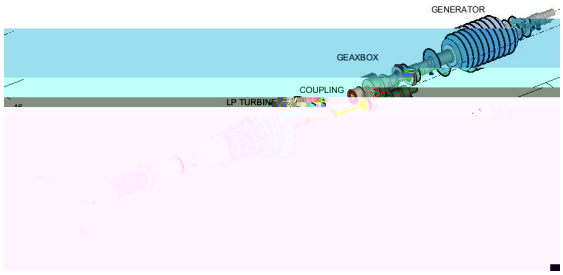

4

2

- -

API684

5

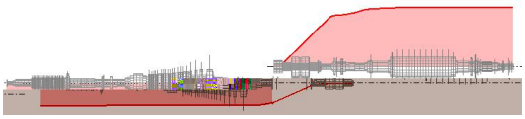

a 12.3Hz

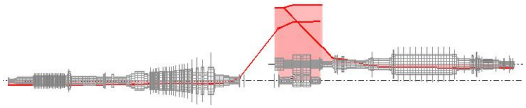

b 55.6Hz

c 114.3Hz

5

API684

10% - -

3

- -

3.1

6 a

6 b 6 c

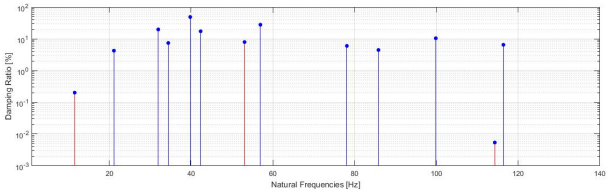

a -

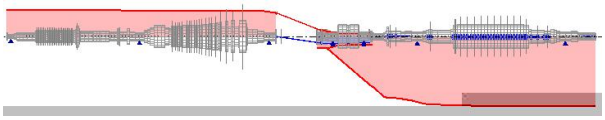

b 11.5Hz

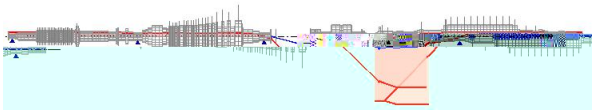

c 53.1Hz

6

6 a

6 a

6 a

6 b 6 c

6 a

6.5

4.5

3.2

ヿ

618000

TK26 A 0001-9006 2022 02-0069-02

Influence of Shaft Sealing Steam Temperature on Unit Startup and Shutdown

WU Wenhua, *LIU Xingbo*, *WANG Wenzhong*, *ZHENG Jian*, *LIU Xiaoyan*, *LIU Xing*

(Dong fang Steam Turbine Corporation, 618000 De yang , Si chuan, China)

Abstract: As one of the important auxiliary systems of the steam turbine, the shaft seal system is mainly used to provide steam source for the shaft seal and recover the steam leakage of the shaft seal and valve under the conditions of steam turbine startup, running and shutdown, so as to prevent the leakage of high temperature and high pressure steam or air into the steam turbine, and affect the vacuum of the unit. This paper mainly introduces the influence of shaft sealing steam temperature on unit startup and shutdown.

Key Words: shaft seal steam delivery; start up; shut down

[2]

[1]

1

1

2021-10-11

1987 2013

1983 2006

1967 1988

1990 2012

1984 2006

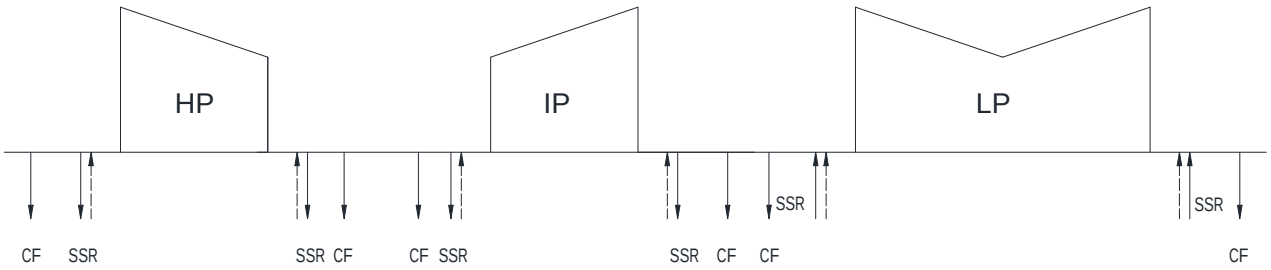

1

2

δ

-

611731

“ ”

-

TM611.31 A 1001-9006 2022 02-0071-04

On the Necessity of A Gas-steam Combined Cycle Project in Dongguan

YANG Zhen

(Dongfang Electric Co.,Ltd.,611731,Chengdu,China)

Abstract:In order to implement the requirements of "continuously implementing air pollution prevention and control actions and winning the blue sky defense war" put forward in the report of the 19th National Congress of the Communist Party of China, improve the air quality of the whole city, promote the construction of beautiful Dongguan and promote the green development of Dawan District of Guangdong, Hong Kong and Macao, Dongguan has formulated the action plan for the blue sky defense war of Dongguan in combination with the actual situation of the city. This paper mainly analyzes the necessity of the construction of a gas steam combined cycle project in Dongguan.

Key words: blue sky defense; power gap; comprehensive utilization of energy; power supply support capability

1

1.1

2035 2050

[1] “ ”

2×460 MW (F) 11

6

8

2021-10-25

(1982) 2005

8

2018 7 790.22 MW 7 425 MW ( )365.22 MW 2018 806.64 kWh 6.04% 15 516.8 MW 3.03% 787.8 kWh 4.51% 15 545 MW 3.91%

1.43 kWh 567.66 kWh 138.93 kWh 98.62 kWh 0.177 2% 70.3734% 17.223 3% 12.226 0% 3.36% 6.01% 7.20% 4.69%

1.2

[2-3]

2020 18 650 MW “ ” 9% 2025 00 MW “ 2.4% 20 22 000 MW ” 1.4% 1

1

	2015	2020	2025	2030
( )				
	12 990	18 650	20 500	22 000
(%)		7.5	2.4	1.4

2020 2025 2030 “ ” “ ” “ ”

2020 2025 2030 5 174 MW 5 740 MW 6 160 MW 2020 2025 2030 3 272 MW 3 616 MW 3 903 MW 2

2 MW

	2015	2020	2025	2030
	/	5 174	5 740	6 160
(%)		/	2.1	1.4
	/	3 272	3 616	3 903
(%)		/	2.01	1.53

1.3

1

~

2022 2025 2030

15 749 MW 16 399 MW 18 124

MW 2022 2025 2030

15 422 MW 16 072 MW 17 797

MW

2

2.1

60t/h

2.2

2 460 MW -

m ψ o

2

2 460 MW -

2022 2025
2030 15 422 MW 16
072 MW 17 797 MW
3 756 MW 2 879 MW 3 299 MW
555 MW 766 MW 1 053 MW
“ ” “ ”

“ ”

3

SO_2 NO_x
80%

SO_2 NO_x

4

4

[1] , , .
[J]. , 2021, 15(3):69-73
[2] , , . [J]. ,
2020,29(1):54-57
[3] , , .
[J]. , 2020, 28(4):90-96
[4] . [J]. , 2020(4):
309-314
[5] , , . [J].
, 2016, 29(1):9-11

上 70

DCS

4

[1] , , . 1 000 MW
[J]. , 2016, 49(6):43-47
[2] , . 600 MW [J].
, 2015, 37(6):62-63+71+79

618000

TM312 A 1001-9006 2022 02-0075-03

Research of High-capacity Bulb Hydro-generator Non-rotational Symmetrical Rotor Bracket

WANG Jiankang, *DU Fangmian*, *LIU Zheng*

(Dongfang Electric Machinery Co., Ltd., 618000, Deyang, Sichuang, China)

Abstract: In this paper, to design rotor bracket of the bulb hydro-generator with special pole number, the concept of non-rotationally symmetric rotor bracket is proposed, and verified by the finite element analysis. Finally, the design principle of the rotor bracket is put forward, which has guidance significance for the design of large-capacity bulb hydro-generator rotor bracket.

Key words: bulb hydro-generator; non-rotationally symmetrical; rotor bracket; design principle

,

1

1.1

40

10 20 40

4 2 1

2021-10-28

1985

1975

1984

2

	MPa	MPa
17 ( )	84	163.3
22 ( )	43	
17 ( )	532	490
22 ( )	404	

2.2

Q345 S-N

17

4 , 40

22

400

2.3

22

500 ,

,

3

2~4 1

(1)

$$Nj \quad N / a.....t \qquad (1)$$

:

*N*j:

N:

a: 1 2~4

t: 1 2

*N*j

t 1 58

58/3=19 1

19 1 4

18 3

t 2 68

68/3=22 2

22 180°

2 4

*N*j+1

t : 1 1

2

*N*j-1

t 1 58

58/3=19

1

18 4 4

14 3

[3] 4

t 2 68

68/3=22 2

21 5 4

16 3 5

16

t 1

t 2

下 80

550000

TV734.1 A 1001-9006 2022 02-0078-03

Discussion on the Feasibility of Hydraulic Turbine Servomotor Transformation in Some Hydropower Station

LIU Daishan

(SPIC Guizhou Jinyuan Co.,Ltd., 550000, Guiyang, China)

Abstract: The hydropower station is located in Shizhu County, Chongqing City. The turbine is equipped with two sets of straight cylinder servomotors with single casing. After a period of operation of the unit, there is oil leakage between the push rod and the casing. With the extension of operation time, the oil leakage is more serious. After analysis, it is proposed to carry out technical transformation of the servomotor and adopt new seals and new structures to solve the oil leakage problem of the servomotor.

Keywords: servomotor; new structure; technical transformation

1.86×10^8 m^3,

117 m

35 MW 70 MW

50 MVA 10.5/110 kV 110 kV “ ” [1]

“ ”

1

“ ”

“ ”

“O”

“O”

2022-04-20

1972 1994

1

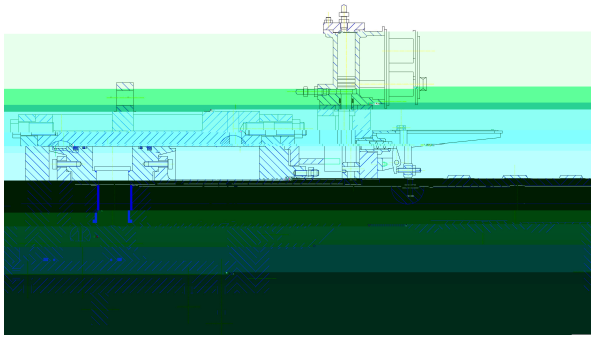

1

2

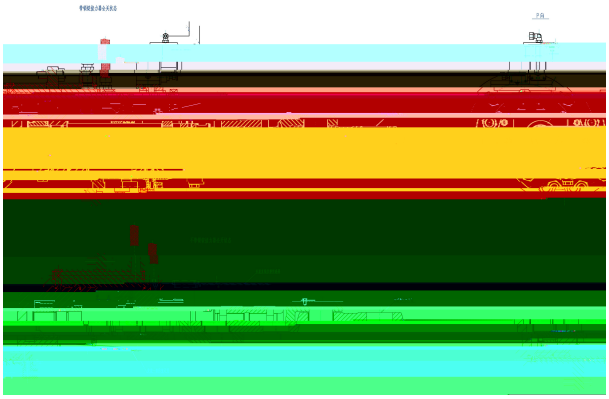

2

6.3 MPa 16 MPa

3

2

[2]

4

[1] . [J]. , 2017, 19(11):27-29

[2] . [J]. , 2013(1):49-51

上 77

4

“ ”

” ” ’€) ” ”)

550000

2007 4 27 2011 2 A

2020

2020

1.1 1

1

		HLD41-WJ-81
	kW	2 632
	m^3/s	5.08
	m	61.57
	m	59.5
	m	58.6
	r/min	750
	r/min	1421
	t	9.5 11.4
	cm	81

1.2 2

2

		SFW2500-8/1730
	kW	2 500
	kVA	3 125
	V	6 300
	A	286.4
		0.8
	r/min	750
	r/min	1 421
		3
		Y
		F/F
	Hz	50

2 1#

1# 2007 4 27

2011 2

A

500 kW 60

1 2011 11

1.8 mm

1#

1

2 ,

3

1.8 mm

1#

1#

2 000 kW 2 340 KW

6

2016 3

2020 1

3

1#

1

2

3

4

5

Â

Ÿ;;; ˇ Ð ˇ ч β °° L ˘ L

U ч A ќ˘ ќ ŋ Н

ˇ˘ ˇ Й, ш̄ ƀ˘ Ỿ

ˈ ʒ˘ ŋ ƀ ɢ 2020 3 ˘ U

Ø˗ ╠ Ỿ ė Â

4

2011 1# ќ ╠ ₹ ʒ ч 2 500 KW˘

ќ U ₹ ʒ 2 340 KW˘ ќ¸ ƨ ĭ

˘ Ӟ. . ⌠

˘ ɢ ضٍ ˘ ₹ ʒ. ч 2 340

KW Â

˘ w □

ĭ *E=γQH* ң ỵ ң ч ˘

ضٍ Ţ w ˘ ỉ ˘ ˆ

№ ч;;;; '

ˆ 1˜ № ˋ à ƀ

ƀ w Й, Â

ˆ 2˜ ˗ №ė ᵩ № ˗ ˘

ɢ ѧ Â

ˆ 3˜ ʒ ˘ h №Â

ʒ ĭ №ч ƀ Re ˆ

ė ᵪ ’ ƀ Re ˆ Ɗρ ė ₹o

˗ ʒ [1]Â ɢ ќ ч β ضٍ o

˘ ƀ. ѵ ϑ ₹o Ɗρ ė ₹o ˗

ʒ ˘ ғ ү ϑ ˘ ⫫

ϑ ж Â Й,

ˆ 1˜ [1]

η_x=ˆ V_2^2-V_5^2˜ /2g-∑h_{2-5} /(V_2^2/2g) ˆ 1˜

V_2---- o

V_5---- ₹o

ɢ o ˘ ⋮ ˘

o V_2 ˘ ү ϑ Â

5

╠ № ˘ ϑ˘ ₹

o Ɗρ ė ₹o ˗ ʒ à ж

ė ж ˘ ₹ ʒ ė

Â1# 72 h ˘ Ỿ ш

⌠ ж ‰ ˘ ₹ ʒ ⌡ 2 850

kW˘ ќ ╠ ѵ 500 kW˘ ĭ r ă

3 ė 4'

3

˜		ч β		25%Ne	50%Ne	75%Ne	100%Ne
1	˘	%	8.1	37.2	53.8	69.2	82
2	;;;	β	m	327.8	327.8	327.8	327.8	327.8
3		β	m	263.9	263.9	263.9	263.9	263.9
4	╠	˗	ώ	0	0.028	0.019	0.023	0.013
5	╠	˗	ώ	0	0.001	0.002	0.003	0.003
6	╠	h ˗	ώ	0	0.003	0.001	0.001	0.001
7	U	˗	ώ	0	0.023	0.024	0.025	0.021
8	U	˗	ώ	0	0.004	0.006	0.008	0.007
9	U	h ˗	ώ	0	0.011	0.007	0.009	0.009

4

˜		ч β		25%Ne	50%Ne	75%Ne	100%Ne
1	ʒ	Ņ	17.5	30.2	30.9	34.6	37.8	38.6
2	╠	Ņ	16.3	34.9	34.9	35.6	38.5	39
3	U	Ņ	14.7	40.4	40.8	40.8	40.7	40.7
4		Ņ		46.3	49.5	49.7	52.1	55.7

6

Ɒ 1# ɢ ќ U Ỿ

h ă ш ƀ ė ˘

˘ ₹ ʒ. ƀ ˘ ˜ № ˘

₹ ˘ ˚ Ð

˘ ќ U ₹ ʒ ⌡ ė ˘ Ỿ

˗ ỵ п ɢ ˘ ᵯ ═ ϑ ᵮ

˘ □ ᵪ ĭ ш̄ Ş ƀ Â

[1] , . ʌ ĭ ʒ [M]. ч ₹ ,

1991

1, 2 1, 2 1, 2 1, 2 1, 2 1, 2

1. 611731 2. 643001

TM615 A 1001-9006 2022 02-0084-05

The Study of the High Temperature Heat Insulation Protection Device of Receiver in the Tower Solar Power Station

DING Lu[1,2], *LIU Yani*[1,2], *HUANG Jibing*[1,2], *CHEN Liang*[1,2], *LIN Yi*[1,2], *SUN Dengke*[1,2]

(1. Clean Combustion and Flue Gas Purification Key Laboratory of Sichuan Province, 611731, Chengdu, China;

2. Dongfang Boiler Group Co., Ltd., 643001, Zigong, Sichuan, China)

Abstract: In the tower solar power station , solar receiver is one of the most important equipment to realize solar thermal power generation. Besides of the effective heating area, the upper, lower and surrounding parts are equipped with high temperature heat insulation protection devices, whose function is to ensure the absolute safety of the internal support structure of the receiver, the system and equipments or the maintenance personnel during operation, so as to avoid the high temperature radiation caused by the overflow light spot reflected by the heliostats field. The design, material and structure of high temperature heat insulation protection device are directly related to the safety, stability and efficient operation of the receiver.

Key words: receiver; high temperature radiation; heat insulation protection

[1]

2022-04-20

1983 2008

1.2

2

, ,

[2-4]

-

1

1.1

2

1

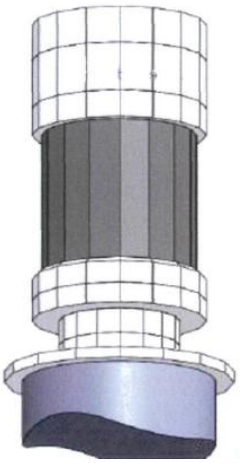

1

2

[6]

[5]

1 2

1

			650	1 000
	kg/m³		220 240	220 270
	MPa		≥ 0.65	≥ 0.65
	MPa		≥ 0.33	≥ 0.33
	%		≤ 2.0	≤ 2.0
	%		≥ 98	≥ 98
		400	≤ 0.100	≤ 0.100
W/m · K		600	≤ 0.130	≤ 0.130
		MPa	≥ 0.4	≥ 0.4
16h		MPa	≥ 0.35	≥ 0.4

GB/T10699-2015

[7] 650 1 000 ,

98%

2

		1 260	1 400	1 400
	kg/m³	≥ 280	≥ 280	≥ 280
	%	≤ 2.5	≤ 2.5	≤ 2.5
At( )	×24h	1 100	1 200	1 200
	%	≤ 1	≤ 1	≤ 1
	%	≤ 1	≤ 1	≤ 1
	MPa	≥ 0.65	≥ 0.65	≥ 0.65
	W/m · K	≤ 0.135	≤ 0.135	≤ 0.135
	500			
	Al_2O_3	≥ 43	≥ 50	≥ 35
%	SiO_2	≥ 55	≥ 48	≥ 48
	Al_2O_3+ SiO_2	≥ 99	≥ 99	——
	Zr O_2	——	——	≥ 15

3

3.1

3

[8]

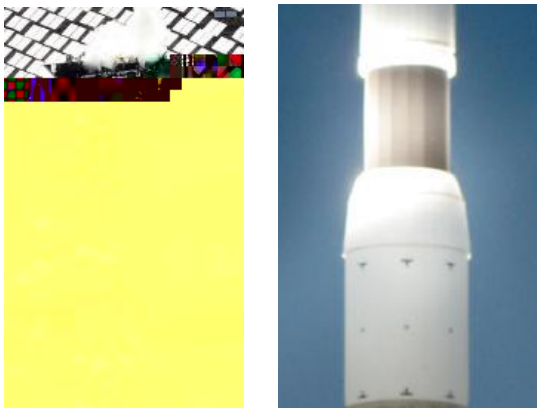

3

4

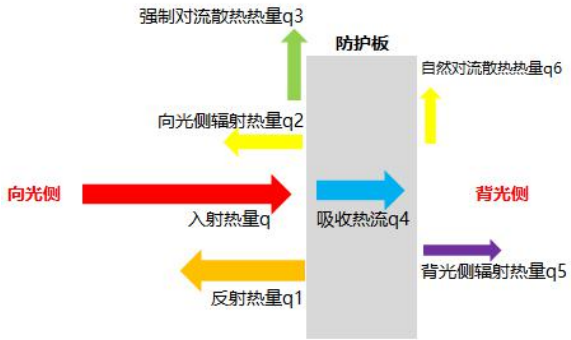

4

q q_1

q_2

q_3

q_4

q_4

q_6

q_5

$$q=q_1+q_2+q_3+q_4 \quad (1)$$

$$q_4=q_5+q_6 \quad (2)$$

ρ ε

q_1 q_2 q_4

ρ ε

q_3

$$V_H = V_{10}(\frac{H}{10})^{\alpha} \quad (3)$$

V_{10}- 10m m/s

V_H- m/s

| -

3

[9]

$$Nu=0.664Re^{1/2}Pr^{1/3} \quad (4)$$

Nu-

Re-

Pr-

q_4

$$q_4 = A\frac{\lambda(Tw-Ti)}{\delta} \quad (5)$$

A , m^2

λ W/ m·K

Tw Ti

| mm

q_6

$$Nu = C(Gr\,Pr)^n \quad (6)$$

C n -

Gr-

Pr-

5

kW/m^2

( )

ρ(0.75 0.8)

400 kW/m^2

800~900

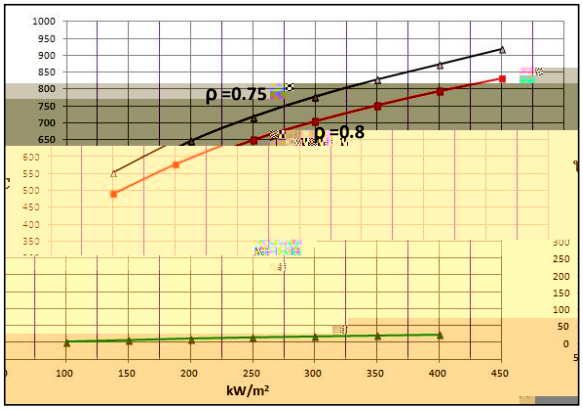

5

3.2

1/2

40°